# Liver Tumor I: Benign Tumors and Tumor-Like Lesions

16

Wilson M. S. Tsui, Takahiro Mori, and Masaki Iwai

## Contents



## Abbreviations

| | |
|---|---|
| AFP | Alpha-fetoprotein |
| AML | Angiomyolipoma |
| BDA | Bile duct adenoma |
| CEA | Carcinoembryonic antigen |
| c-myc | Cancer-myelocytomatosis |
| ELISA | Enzyme-linked immunosorbent assay |
| FNH | Focal nodular hyperplasia |
| HCA | Hepatocellular adenoma |
| HCC | Hepatocellular carcinoma |
| HMB45 | Human melanoma black 45 |
| HNF-1 | Hepatocyte nuclear factor 1 |
| IL6ST | Interleukin 6 signal transducer |
| IPN | Intraductal papillary neoplasm |
| IPT | Inflammatory pseudotumor |
| L-FABP | Liver fatty acid binding protein |
| LMS | Larva migrans syndrome |
| MCN | Mucinous cystic neoplasm |
| p53 | 53-kilodalton protein |
| PECOMA | Perivascular epithelioid cell tumors |
| PIVKA2 | Protein induced by vitamin K absence or antagonist-2 |

W. M. S. Tsui, MD, FRCPath (✉)
Hong Kong, China
e-mail: mstsui@ha.org.hk

T. Mori, MD, PhD
Hyogo, Japan

M. Iwai, MD, PhD
Kyoto, Japan

Compared to malignant tumors, benign tumors of the liver are encountered rarely in daily practice, although their true incidence is probably not low [1]. This is because they are either asymptomatic and not discovered or they are not biopsied and



E. Hashimoto et al. (eds.), *Diagnosis of Liver Disease*, https://doi.org/10.1007/978-981-13-6806-6_16

left unresected. However, ultrasonographic imaging often may show benign tumors in the liver. Some of these tumors are true neoplasms, while others are tumor-like masses (Table 16.1) [2].

## 16.1 Hemangioma

Hemangioma is the most common benign tumor of the liver, being noted in 0.4–20% of cases in autopsy studies. The asymptomatic lesions are usually solitary and are typically <5 cm in diameter. Patients sometimes present with abdominal pain or discomfort and a palpable mass. Large tumors may rarely be complicated by rupture, thrombocytopenia, and consumptive coagulopathy (Kasabach-Merritt syndrome) [3]. A large or ruptured hemangioma requires immediate surgical intervention.

**Table 16.1** Benign neoplasms and tumor-like lesions of the liver

| Tumor | Lesion |
|---|---|
| Hepatocellular tumors | Focal nodular hyperplasia |
| | Hepatocellular adenoma |
| Biliary tumors | Biliary microhamartoma (von Meyenburg complex) |
| | Bile duct adenoma |
| | Biliary adenofibroma |
| | Mucinous cystic neoplasm (biliary cystadenoma) |
| | Intraductal papillary neoplasm (biliary papillomatosis) |
| | Other pancreatic type tumors |
| Vascular tumors | Hemangioma |
| | Infantile hemangioma |
| | Lymphangioma and lymphangiomatosis |
| Miscellaneous tumors | Angiomyolipoma and lipomatous tumors |
| | Leiomyoma |
| | Solitary fibrous tumor |
| | Mesenchymal hamartoma |
| | Benign teratoma |
| Miscellaneous lesions | Inflammatory pseudotumor |
| | Fibrosing necrotic nodule |
| | Parasitic granuloma |
| | Nodular transformation |
| | Pseudolipoma |
| | Heterotopia (adrenal, pancreas, spleen) |
| | Gauzeoma |

Histologically, liver hemangioma is mainly cavernous type. Complications such as thrombosis, infarction, sclerosis, and calcification may occur, leading to possible confusion with a more aggressive tumor. Although hemangiomas are grossly well circumscribed, microscopic extension of dilated vascular spaces into adjacent hepatic parenchyma may be observed [4]. Though extremely rare, diffuse and multiple lesions occur with progressive development [5], and some cases are associated with bone and lung involvement (diffuse systemic hemangiomatosis). Multiple or diffuse lesions must also be differentiated from peliosis hepatis and hereditary hemorrhagic telangiectasia. Recently a rare small vessel-type hemangioma with infiltrative border is recognized and has to be distinguished from angiosarcoma by immunohistochemical staining for p53, c-myc, and Ki-67 [6].

Hemangiomas are usually asymptomatic. The diagnosis is based on imaging studies. Abdominal ultrasonography (US) shows a hyperechoic structure with smooth margin; CT reveals hypodense tumor; and CT with contrast medium shows enhanced tumor in a peripheral-central direction with focal globular pattern. MRI displays low-signal T1 time and hyperintensity in the T2-weighted image. Sclerosed hemangioma has atypical imaging features and may be confused with hepatocellular carcinoma, cholangiocarcinoma, and metastatic tumor [7].

### Case 16.1

A 51-year-old female complained of persistent right flank pain, and her ultrasonographic diagnosis was liver hemangioma. Her liver function test showed TBIL 0.92 mg/dL, AST 12 IU/L, ALT 12 IU/L, LDH 197 IU/L, and AFP 1.6 ng/mL. HBsAg and anti-HCV were negative. Computed tomography (CT) showed a low-density signal in the S6 area and enhancement on the edge of the tumor in the arterial phase (Fig. 16.1). The tumor had a larger circumference in the venous phase, and low density remained in the center. T1 image on magnetic resonance imaging (MRI) showed a low-intensity area in S6, MRI with

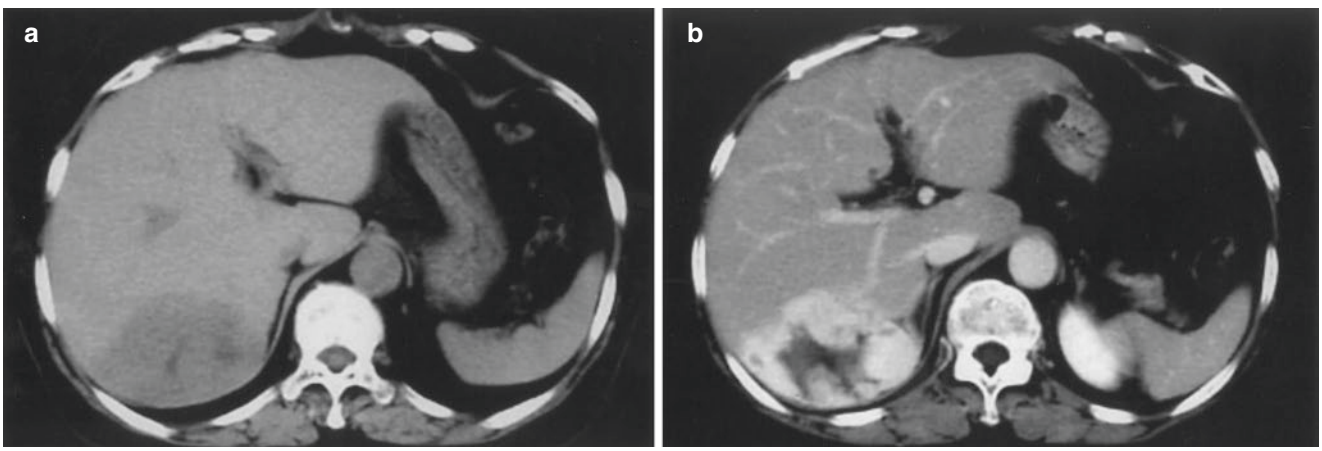


**Fig. 16.1** Hemangioma. (**a**) CT without contrast medium shows low-density area in S6. (**b**) Contrast medium is retained from the edge to the center

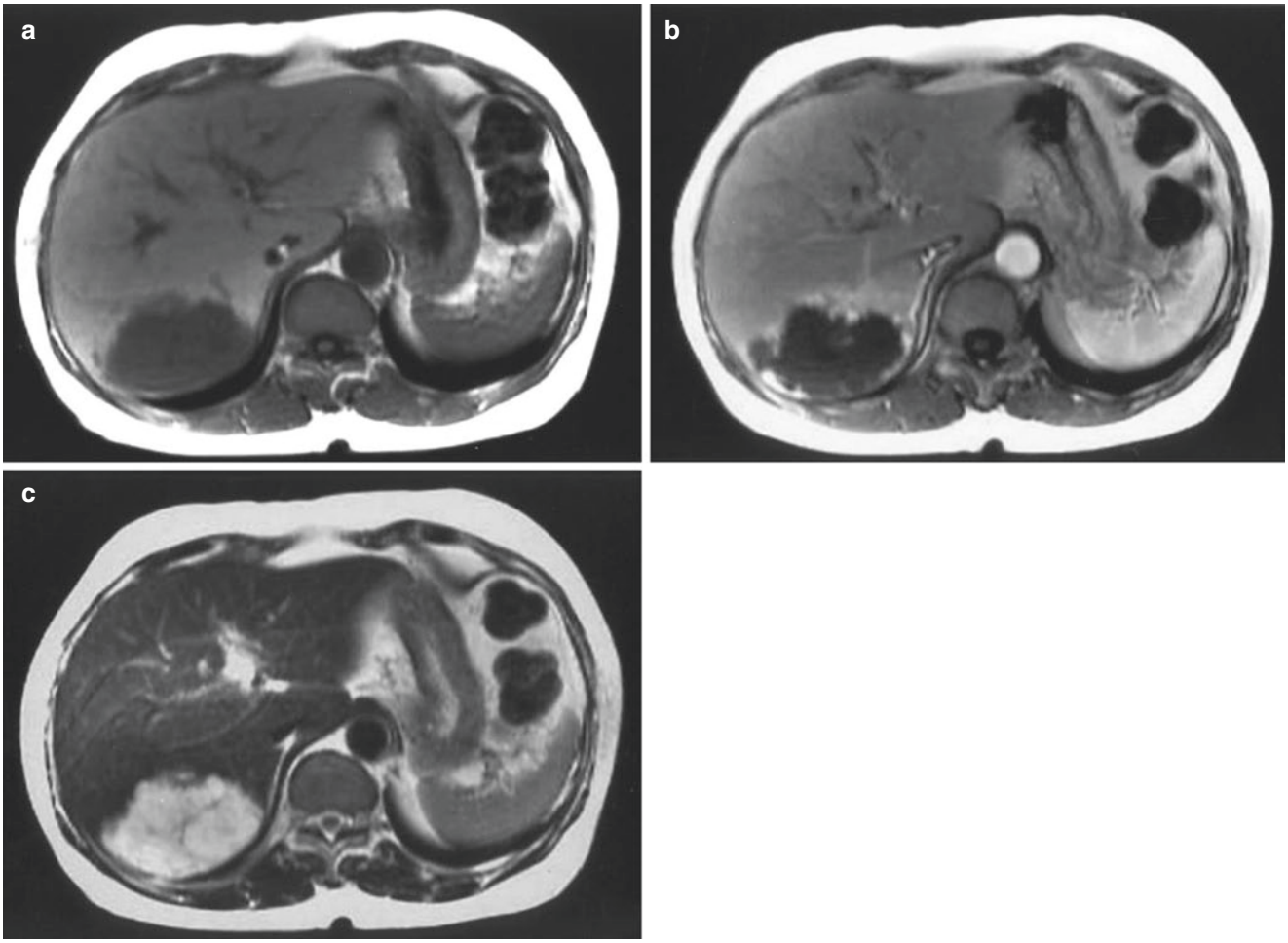


**Fig. 16.2** Hemangioma. (**a**) T1-weighted image on MRI shows low intensity in S6. (**b**) MRI with contrast medium shows high-intensity area on the edge of tumor in early phase. (**c**) MRI with contrast medium reveals high intensity in tumor

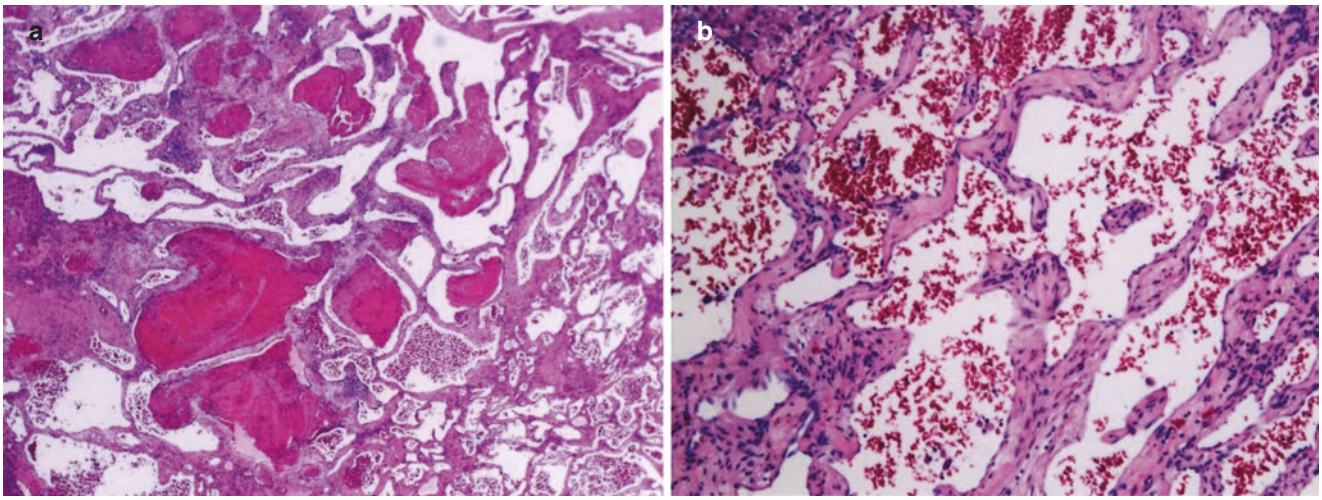


**Fig. 16.3** Hemangioma. (**a**) Histology shows cavernous spaces filled with blood cells. (**b**) Vascular spaces are lined by flattened endothelial cells and filled with blood cells

contrast medium revealed high-intensity area on the edge, and T2 revealed high intensity in the tumor (Fig. 16.2). Surgically resected tissues showed cavernous vascular spaces filled with blood cells or amorphous materials, and the cavernous spaces were separated by delicate fibrous strands and lined by flattened endothelial cells without atypia (Fig. 16.3).

**Case 16.2**

An obese female aged 76 years suffered from diabetes mellitus, and her abdominal CT showed low-density area (25 mm on diameter) in S4, and faint staining was detected in the center of tumor during early and late phase of enhanced CT (Fig. 16.4). All liver function tests were normal, and tumor markers of AFP, PIVKA2, CEA, and CA19-9 were within normal limit. MRI showed low intensity in the tumor by T1 and slightly high intensity by T2, and dynamic MRI revealed low intensity in tumor as well as non-tumor area in early and late phase and slight retention of contrast medium in the center during the late phase (Fig. 16.5). Tumor biopsy under echo guidance revealed small- and variously sized vessels surrounded by thick myxoid walls and lined with flattened endothelial cells. Cavernous formation was not well developed, and red blood cells were scanty in the lumen (Fig. 16.6). The histological features are consistent with sclerosing cavernous hemangioma.

In this rare sclerosing cavernous hemangioma, the lesion cannot be detected as cavernous hemangioma by CT and MR imaging. There have been only a few studies to report radiological findings of sclerosed hemangiomas, and the majority is reported to present as a perfusion defect on enhanced CT [8]. In addition sclerosed hemangiomas exhibit mild to moderate hyperintensity on T2-weighted MR images, hypointensity on T1-weighted images, patchy enhancement during the arterial phase, and gradual enhancement during the delayed phases [9]. Hemorrhage, thrombosis, or infarction within a

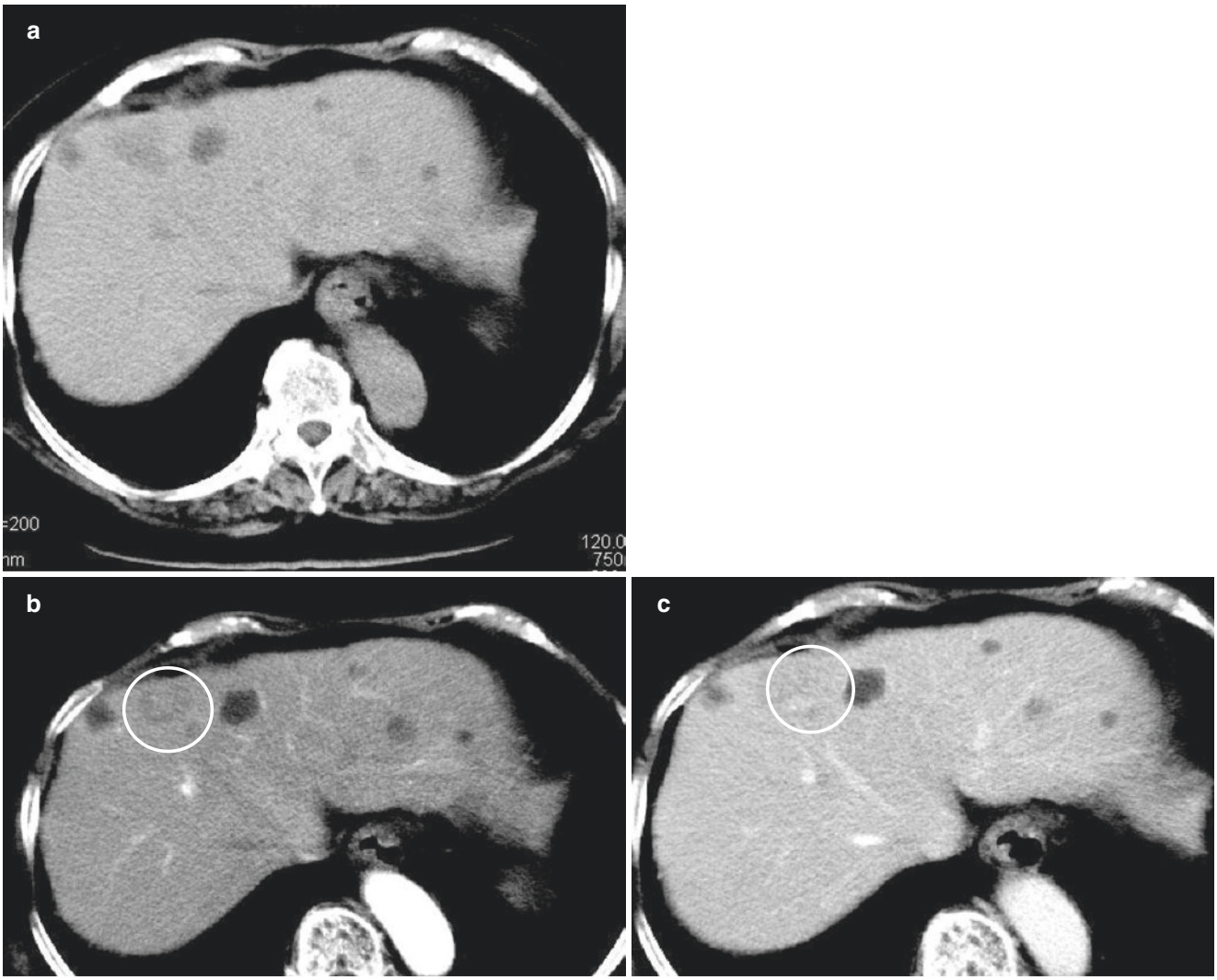


**Fig. 16.4** Sclerosing cavernous hemangioma. (**a**) Low-density area (LDA) (about 2.5 cm in diameter) is seen in S4, and several cystic lesions are seen in both lobes. (**b**) LDA is slightly enhanced from center by contrast medium in early phase. (**c**) Enhancement in center of LDA is retained in late phase

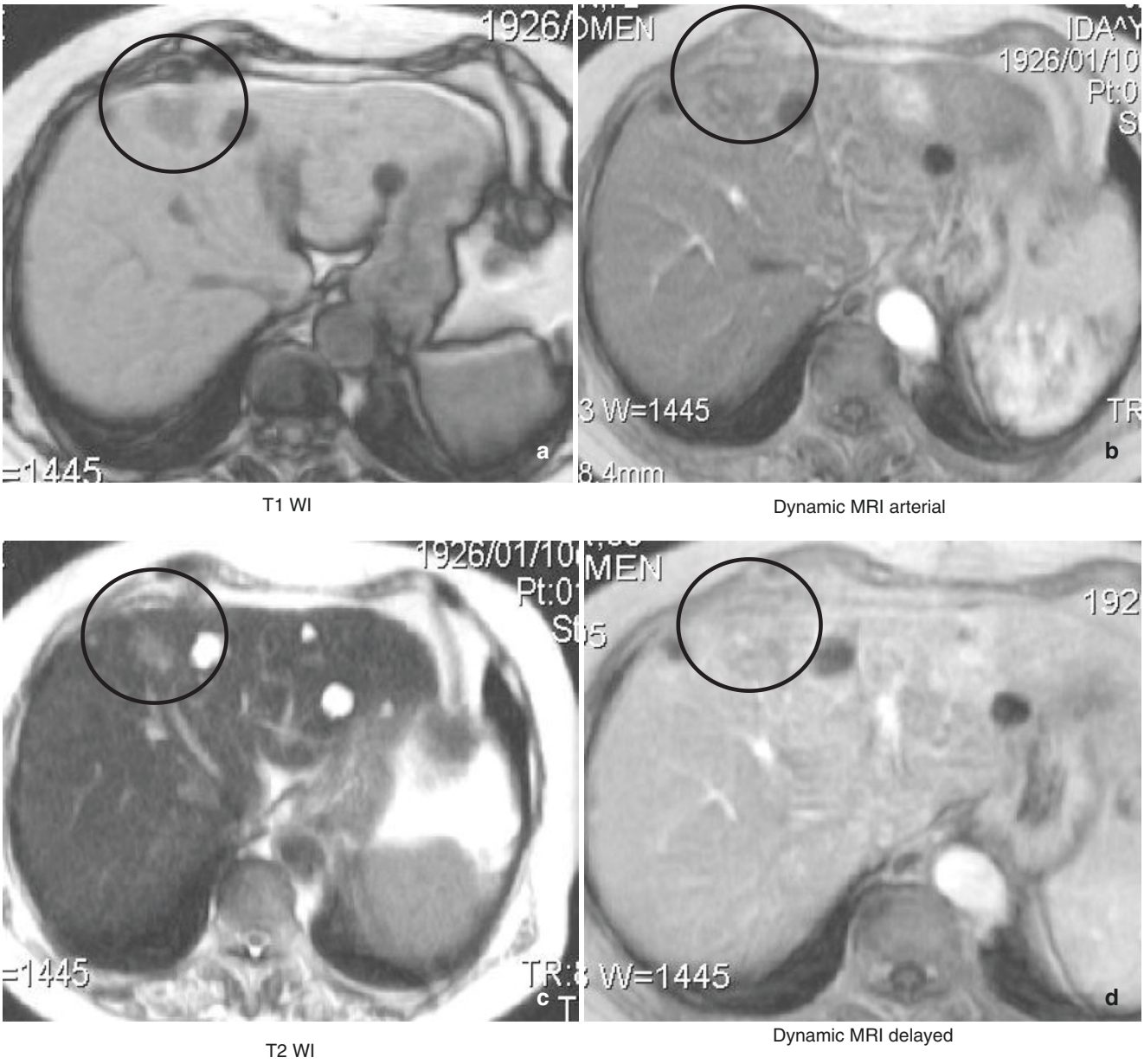


**Fig. 16.5** Sclerosing cavernous hemangioma. (**a**) MRI intensified by T1 shows low intensity in tumor and (**b**) by T2 shows weakly high intensity in tumor. (**c**) Dynamic MRI shows iso-intensity in circumference of tumor in arterial and delayed phase, and low intensity is seen in center, and (**d**) enhancement is seen in center during delayed phase

cavernous hemangioma may instigate progression to a sclerosed hemangioma, as a result of fibrosis and hyalinization of thick-walled blood vessels. Mast cells have been implicated in the development of this process [10].

## 16.2 Focal Nodular Hyperplasia

Focal nodular hyperplasia (FNH) is the second most common benign liver process. It occurs in both sexes and across all ages, but most commonly in young adult women [11]. It is usually solitary but can be multiple in 20–30% of cases. It is usually <5 cm in diameter and discovered incidentally on physical examination or by imaging, but it may also present with complications attributed to large size (or, rarely, due to hemorrhage or pain). Some patients with the so-called multiple FNH syndrome have at least two FNHs associated with one or more lesions, such as hepatic hemangioma, arterial vascular malformations, meningioma, and astrocytoma.

FNH is a polyclonal nonneoplastic lesion [12]. The currently favored hypothesis of its tumorigenesis is that it represents a hyperplastic and altered growth response to changes in blood flow in the parenchyma surrounding a preexisting arterial malformation [13]. The ductular proliferation, once

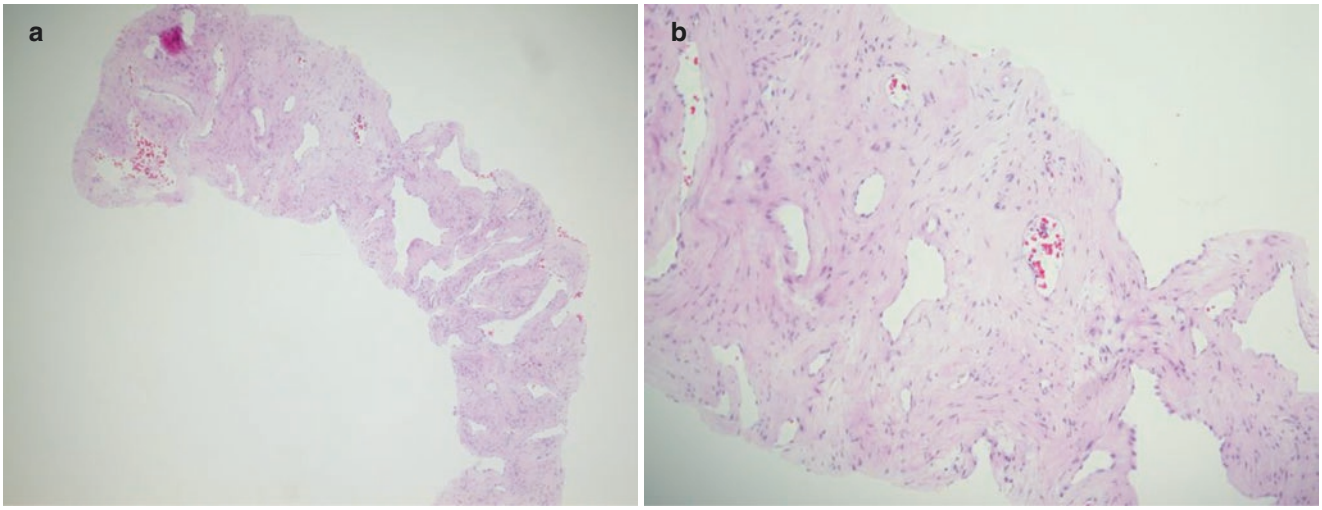


**Fig. 16.6** Sclerosing cavernous hemangioma. (**a**) Blood spaces are separated by broad fibrotic septa. Vessels are generally small in size, and a few of them are dilated. (**b**) Small irregular vessels are lined by flattened endothelium, with small amount of red blood cells in lumen. Fibrotic septa area is broad and myxoid

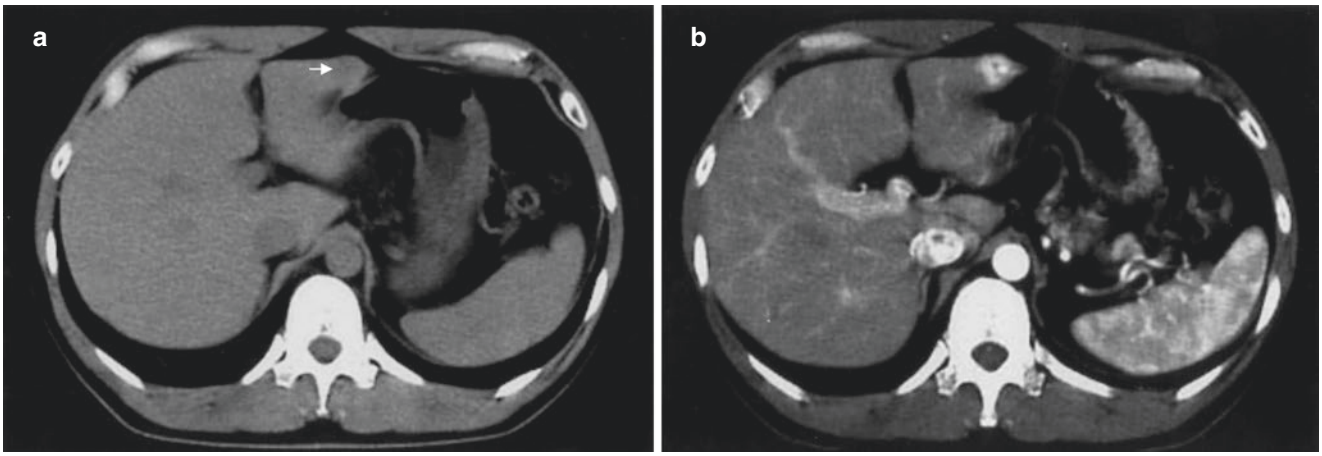


**Fig. 16.7** Focal nodular hyperplasia. (**a**) CT without contrast medium shows small, low-density area (arrow) in S3. (**b**) CT with contrast medium shows enhanced area in the tumor. Its center is more enhanced, mixed with low-density area

thought to arise from biliary metaplasia of hepatocytes, appears to be an attempt to establish biliary drainage, as normal bile ducts are absent and features of chronic cholestasis (pseudoxanthomatous change, copper accumulation) are often present.

FNH is difficult to diagnose on biopsy if the central scar and abnormal vessels are not included in the samples and is frequently mistaken for hepatic adenoma, cirrhosis, or ductopenic syndrome (such as primary biliary cirrhosis). The demonstration of map-like immunostaining pattern of glutamine synthetase overexpression is very helpful for histological diagnosis. A rare variant of FNH, the telangiectatic type, which does not have the central fibrous scar and contains dilated blood-filled vascular spaces, is now regarded as the inflammatory subtype of hepatic adenoma [14, 15].

**Case 16.3**

A 38-year-old man was found to have a liver tumor by abdominal US during a medical examination. His liver function test revealed TBIL 1.1 mg/dL, ALT 27 IU/L, AST 22 IU/L, ALP 227 IU/L, CEA 1.4 ng/mL, and negative AFP. Both HBsAg and anti-HCV were negative. CT without contrast medium showed low-density area in S3, and CT in the arterial phase showed enhanced tumor in S3 with a densely stained center (Fig. 16.7). MRI T2-weighted image showed high-intensity area in S3 (Fig. 16.8). Angiography revealed tumor stain with radiating artery in the center in arterial phase, and it remained in the late venous phase (Fig. 16.9). Resected liver tumor showed well-demarcated, unencapsulated lesion with nodular appearance (simulating cirrhosis), pale color, and central fibrous scar. Microscopy revealed

central scar formation with abnormal thick-walled muscular vessels and radiating fibrous septa; there were proliferating bile ductules, infiltration of inflammatory cells, and dilated vessels between septal fibrosis and nodule formation (Fig. 16.10). Hepatocytes were arranged in liver plates of normal or slightly increased thickness. No cirrhotic change was seen in non-nodular area.

## 16.3 Hepatocellular Adenoma

Hepatocellular adenoma (HCA) is a rare tumor seen almost exclusively in young women during their reproductive years and rarely in men or children. It can be single or multifocal; the latter condition is known as multiple hepatocellular adenomatosis. The general clinical presentation is an abdominal mass, but some patients also complain of abdominal pain, discomfort, or nausea, and a significant number present with hemoperitoneum. Serum alkaline phosphatase may be elevated, but serum alpha-fetoprotein levels are generally normal or minimally elevated. On radiography, the lesions show increased vascular pattern.

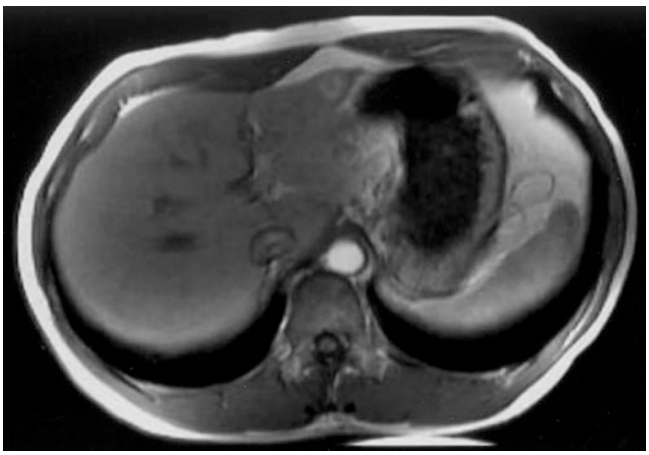

**Fig. 16.8** Focal nodular hyperplasia. T2-weighted image on MRI shows high-intensity area in S3

HCA is strongly associated with oral contraceptive use and androgen steroid therapy, and occurs in a liver that is histologically normal or nearly normal. It can also occur spontaneously or be associated with underlying metabolic diseases, including type I glycogen storage disease, galactosemia, tyrosinemia, and familial diabetes mellitus. There is a significant risk of serious complications, such as hemorrhage and rupture. HCC is rarely found to arise from HCA, and this risk is higher in males and with large adenomas. Surgical resection is recommended if there is no tumor regression after the cessation of oral contraceptive use.

It has been observed recently that HCAs are heterogeneous with regard to their phenotypes and genotypes [16], based on which a new pathomolecular classification was proposed [17]. At least four subtypes are described:

1. HNF1-alpha-mutated adenomas, which account for 40% of adenomas, are characterized by prominent steatosis and negative expression of liver fatty acid binding protein (L-FABP).
2. Beta-catenin-mutated adenomas, which are preferentially encountered in male patients, are morphologically characterized by the presence of cellular atypia, association

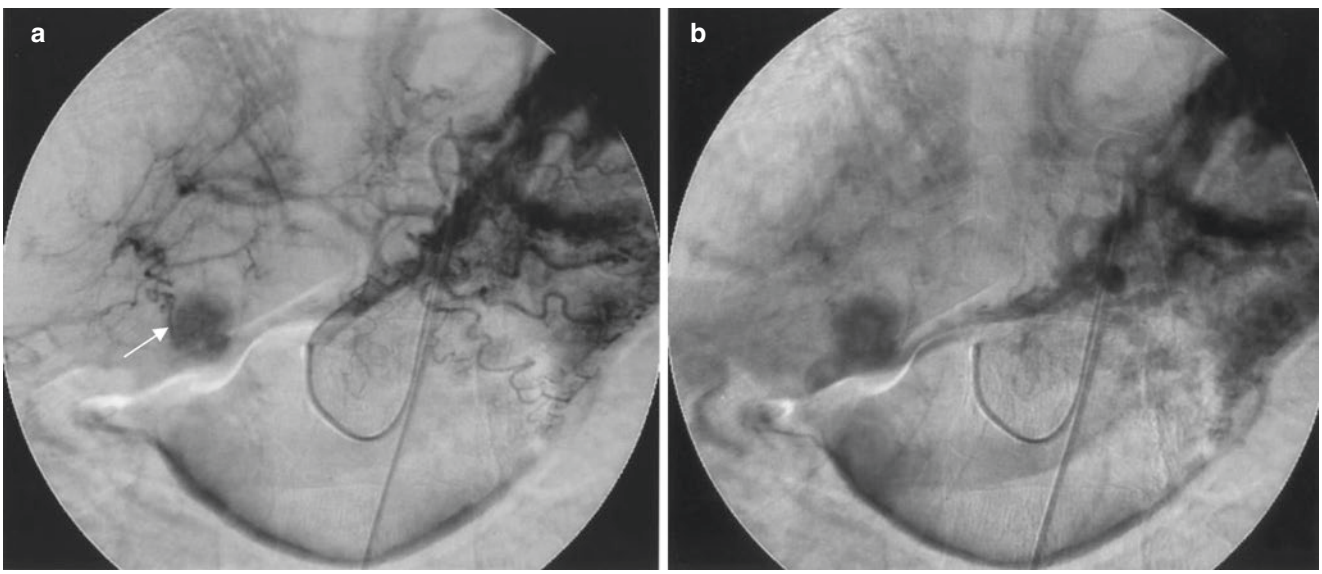


**Fig. 16.9** Focal nodular hyperplasia. (**a**) Angiography shows stain with radiating vessels in tumor (arrow). (**b**) Tumor stain is retained in the late stage of venous phase

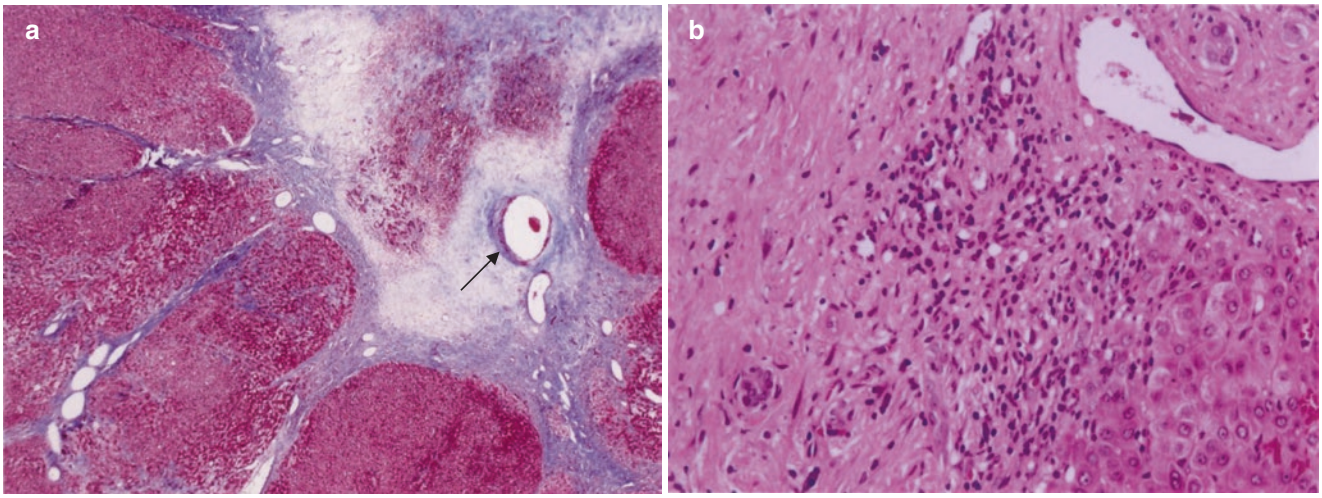


**Fig. 16.10** Focal nodular hyperplasia. (**a**) Masson trichrome stain shows central stellate fibrous scar extending to the periphery and separating nodules. Arterial vessel (arrow) is seen in center of scar. (**b**) Infiltration of lymphocytes, proliferating bile ductules, and dilated vessels between radiating fibrosis and nodule formation are seen

with a higher risk of malignant transformation, and nuclear expression of β-catenin and overexpression of glutamine synthetase.
3. Inflammatory adenomas, which are related to mutations in the IL6ST gene, frequently display telangiectasia and inflammatory infiltrates and characteristically show positive immunostaining with markers of the acute-phase inflammatory proteins such as serum amyloid A (SAA) and C-reactive protein (CRP).
4. Unclassifiable adenomas without any specific clinical, morphological, or genetic characteristics.

Diagnostic problems arise most often in the differentiation of HCA from FNH or well-differentiated HCC, especially when hybrid features are present. Immunohistochemistry is now able to distinguish HA from either of these two lesions.

**Case 16.4**
A 36-year-old lady was found to have liver tumor by US during investigation for dysphagia. She was on oral contraceptives for several years and was also an HBsAg carrier. Her AFP level was not elevated, and liver function was normal. CT with contrast medium showed an isodense poorly enhancing 2.5-cm mass in the right lobe of the liver. Angiography revealed a hypervascular mass with lipiodol uptake and was demonstrated on subsequent CT. With a preoperative diagnosis of HCC, the tumor was resected, and a benign diagnosis was established from frozen section. The specimen showed a subcapsular, ill-defined, and yellowish-brown nodule. It comprised a relatively uniform population of larger and paler hepatocytes arranged in plates one to three cells thick, without free-floating trabecular formation; no capsule was seen between the nodule and non-nodular tissue. Reticulin framework of the cell plates was either intact or only focally decreased. Thick-walled arterial vessels occurred in clusters, and thin-walled venous vessels were scattered throughout (Fig. 16.11). No portal tracts were detected.

## 16.4 Bile Duct Adenoma

Usually an incidental finding at surgery or autopsy, bile duct adenoma (BDA) presents as a solitary subcapsular nodule in 90% of patients. Its main clinical significance resides in its possible confusion with adenocarcinoma at laparoscopy or laparotomy.

BDA consists of a small (≤1 cm) disordered collection of ductules in connective tissue stroma showing varying degrees of chronic inflammation and collagenization, with occasional portal tracts enclosed in the nodule. Mucinous metaplasia, alpha-1 antitrypsin droplets, and neuroendocrine differentiation may be seen in the tubular lining cells.

The origin and pathogenesis of BDA are controversial. In early literature, it was regarded as a true neoplasm [18], but this view has been rejected. Researchers have proposed that it is a localized ductular proliferation following a focal injury or a form of peribiliary gland hamartoma [19, 20].

**Case 16.5**
A 43-year-old man was on follow-up for hepatitis B cirrhosis when he was found to have a 2.5-cm HCC during cancer screening. During surgery, another small 8-mm subcapsular nodule was detected and submitted for frozen section. Microscopy revealed tubular or curvilinear ductules lined by cuboidal epithelium, embedded in a fibrous stroma with patchy inflammatory infiltrate and some residual portal tracts (Fig. 16.12).

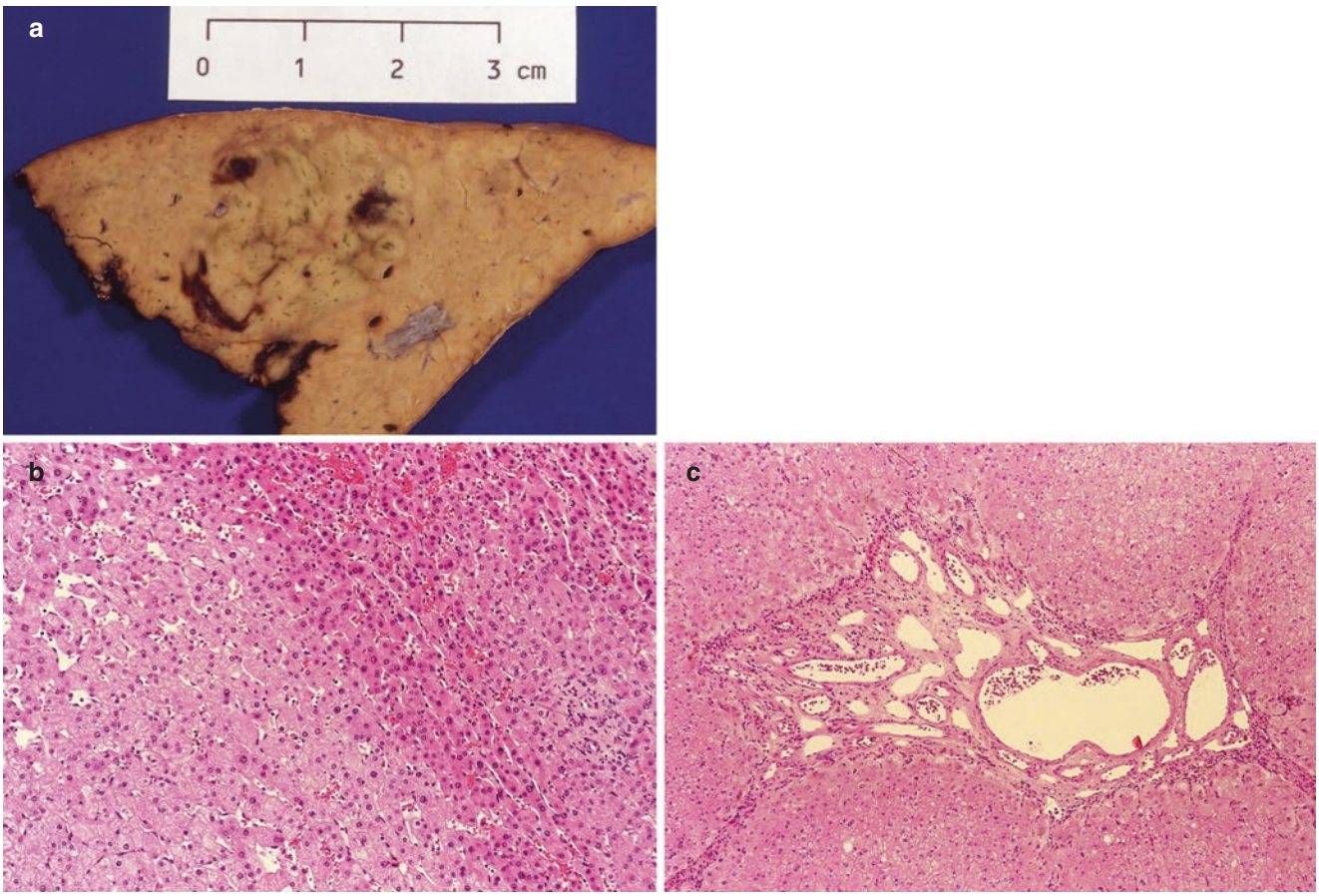


**Fig. 16.11** Hepatic adenoma. (**a**) Resected tumor shows a subcapsular, ill-defined, and yellowish brown nodule. (**b**) Tumor comprises relatively uniform population of larger and paler hepatocytes arranged in cell plates that are one to three cells thick, and no capsular formation is seen in boundary between nodule and normal liver tissue. (**c**) Thick-walled arterial vessels occur in clusters

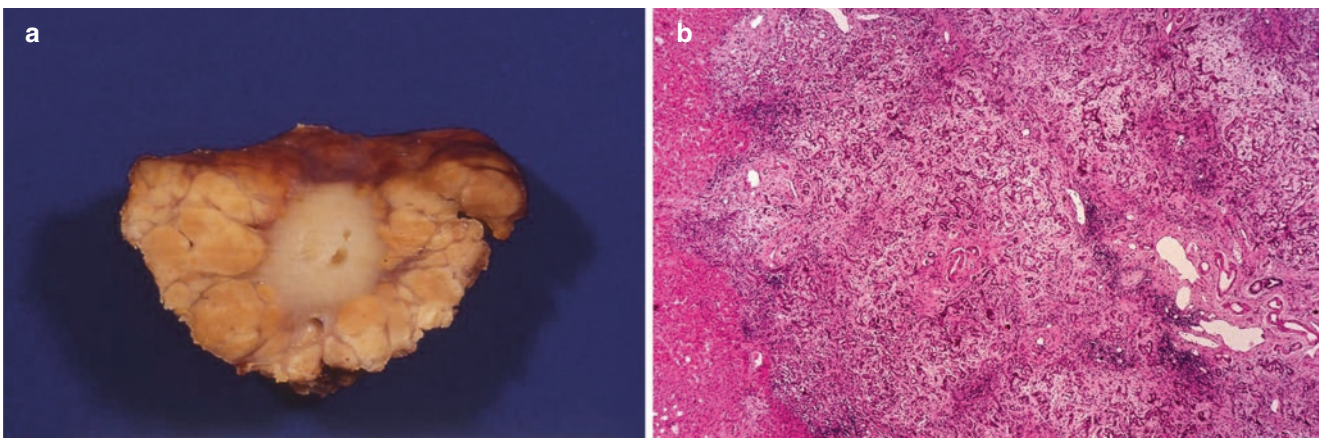


**Fig. 16.12** Bile duct adenoma. (**a**) Resected specimen shows a subcapsular 8-mm whitish nodule against background of yellowish brown cirrhosis. (**b**) Nodule comprises many small ductules in fibrous stroma with patchy inflammatory infiltrate and trapped residual portal tracts

## 16.5 Biliary Adenofibroma

Biliary adenofibroma appears to be an extremely rare type of benign bile duct tumors. Only a few cases have been reported in the literature [21–23]. It is characterized by microcystic and tubuloacinar glandular structures lined by biliary epithelium and supported by fibroblastic stromal scaffolding.

There is evidence that this tumor might originate from preexisting biliary microhamartoma (von Meyenburg complex) based on similar morphological architecture and epithelial expression of D10, but not 1F6 [23]. Due to its size, proliferative activity, and p53 positivity, it is a potentially premalignant lesion [24]. Indeed, cases of malignant transformation are coming up [25, 26]. Another possibly neoplastic form of BDA, "atypical clear cell bile duct adenoma," has also been described [27].

**Case 16.6**

A 74-year-old woman presented with right upper abdominal pain, and US revealed gallstones and round liver mass with homogeneous echogenicity and lobulated border. CT showed hypodense lesion with heterogeneous contrast enhancement due to vessels in portions of the tumor. Laparotomy revealed a 7-cm tumor protruding from the inferior surface of the right lobe. Resected tumor showed honeycomb cut surface with thin fibrous septa delineating small cysts. Microscopically, it comprised acinar, microcystic, and tubuloglandular elements separated in most areas by thin fibrous bands. The lining epithelium consisted of a single layer of non-mucin-secreting flat to cuboidal to columnar cells, with occasional mitoses (Fig. 16.13).

## 16.6 Mucinous Cystic Neoplasm

Mucinous cystic tumor (MCN), previously referred to as biliary cystadenoma, is a solitary and multilocular cystic tumor that arises principally within the liver but may occur in the extrahepatic biliary tree including the gallbladder [28–30]. It has striking similarities to mucinous cystic neoplasm of the pancreas. Both are tumors predominantly found in middle-aged women in >90% of cases. The most common presenting symptoms are upper abdominal mass, discomfort, and pain.

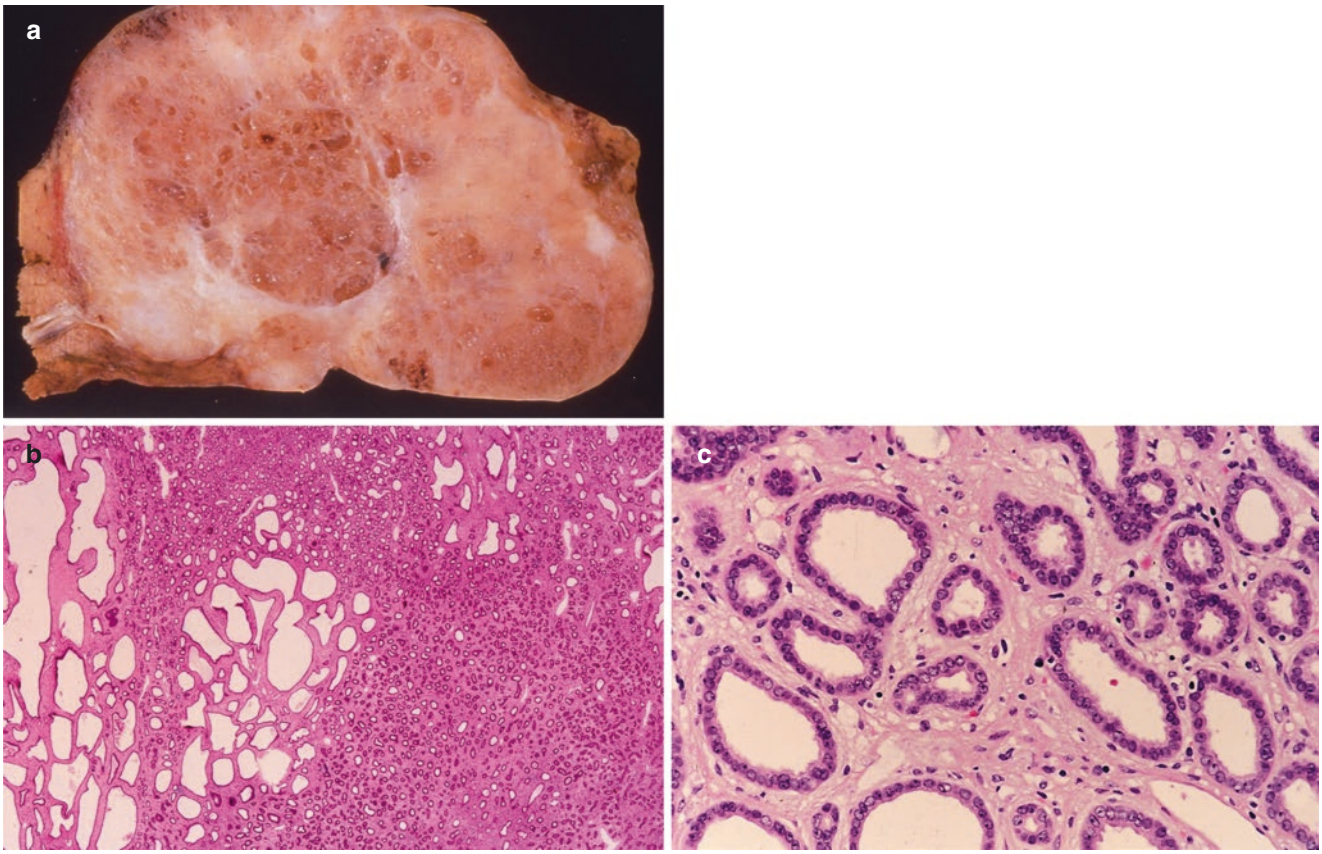


**Fig. 16.13** Biliary adenofibroma. (**a**) Tumor is circumscribed with microcystic cut surface. (**b**) Tumor comprises tubules, acini, and microcysts in fibrotic stroma. (**c**) Lining epithelium has a single layer of cuboidal to columnar biliary-type cells, with occasional mitoses

A slow-growing tumor, MCN frequently reaches a large size and has a tendency to become malignant, usually over a period of many years. Foci of epithelial atypia indicate "borderline" or potentially malignant change. Recurrence is the rule following incomplete excision. Complete surgical removal is mandatory and usually curative.

The origin of MCN remains speculative. Embryonic foregut rests have been suggested as sources of the neoplasms [31]. Considering the site of occurrence, histological morphology, and frequent appearance of endocrine cells, it is likely that MCN originates from peribiliary glands with mucin secretion and cyst formation [32]. However, the female-specific mesenchymal stroma remains enigmatic.

Other pancreatic type tumors are occasionally found in the liver. Serous cystadenoma (microcystic adenoma) and papillary cystic tumor (solid pseudopapillary tumor) have been described [30, 33], and their occurrence has been attributed to pancreatic exocrine acini in peribiliary glands [34].

**Case 16.7**

A 48-year-old woman with a long history of intermittent abdominal pain had recently developed symptoms of indigestion and epigastric fullness. Upper endoscopy was negative for ulcer disease. CT and US of the abdomen revealed a 19-cm cyst in the left lobe of the liver compressing the hilum, gallbladder, and stomach. The resected specimen was a multilocular cyst. The locules were lined by a single layer of mucin-secreting columnar to cuboidal biliary type epithelium; the supporting stroma was compact and cellular, resembling ovarian stroma, and was immunoreactive with estrogen and progesterone receptors and inhibin (Fig. 16.14).

## 16.7 Intraductal Papillary Neoplasm

Intraductal papillary neoplasm (IPN), previously referred to as biliary papillomatosis, consists of multicentric papillary adenomas in the biliary tract, similar to intraductal papillary mucinous neoplasm of the pancreas, although not as commonly mucin secreting [35]. The gallbladder and major pancreatic ducts may also be involved. The adenomatous epithelium shows varying degrees of dysplasia and may mimic biliary epithelium and exhibit gastric or intestinal metaplasia. Based on morphologic characteristics and mucin expression, four subtypes of IPN are defined: pancreatobiliary, intestinal, gastric, and oncocytic. Patients usually present in middle to old age, with a male to female ratio of 2 to 1. The condition is characterized by recurrent bouts of cholangitis and obstructive jaundice. Occasional cases have been associated with ulcerative colitis, hepatolithiasis, Caroli's disease, choledochal cyst, and polyposis coli [36]. Preoperative diagnosis is difficult, but possible, by means of endoscopic retrograde cholangiopathy (ERCP) and endoscopic biopsy for extrahepatic cases and percutaneous transhepatic cholangioscopy (PTC) and fine needle aspiration cytology (FNAC) for intrahepatic tumors [37, 38].

Although histologically benign, its clinical behavior is regarded as having a borderline or low-grade malignant potential [39] due to its tendency to recur, multicentricity, susceptibility to malignant transformation, and significant morbidity and mortality arising from complications like recurrent bouts of cholangitis and obstructive jaundice, as well as episodes of sepsis and hemobilia. Management is difficult, and a cure is unlikely without liver transplantation [40]. Even then, the lesion may recur in the extrahepatic ducts.

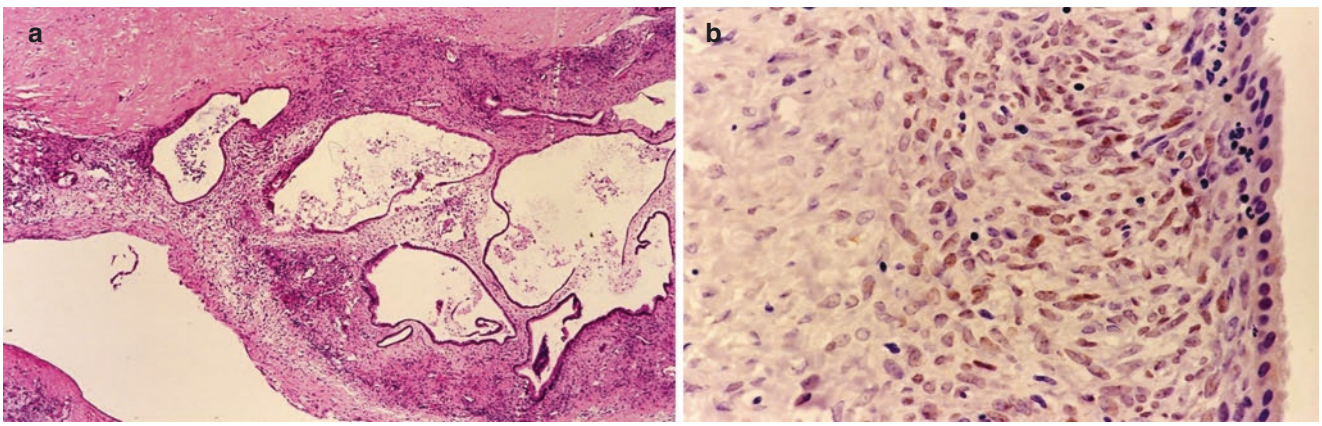


**Fig. 16.14** Mucinous cystic neoplasm (biliary cystadenoma). (**a**) Multicystic locules are lined by a single layer of mucin-secreting epithelium. (**b**) Subepithelial mesenchymal stroma is ovarian-like and expressed estrogen receptor

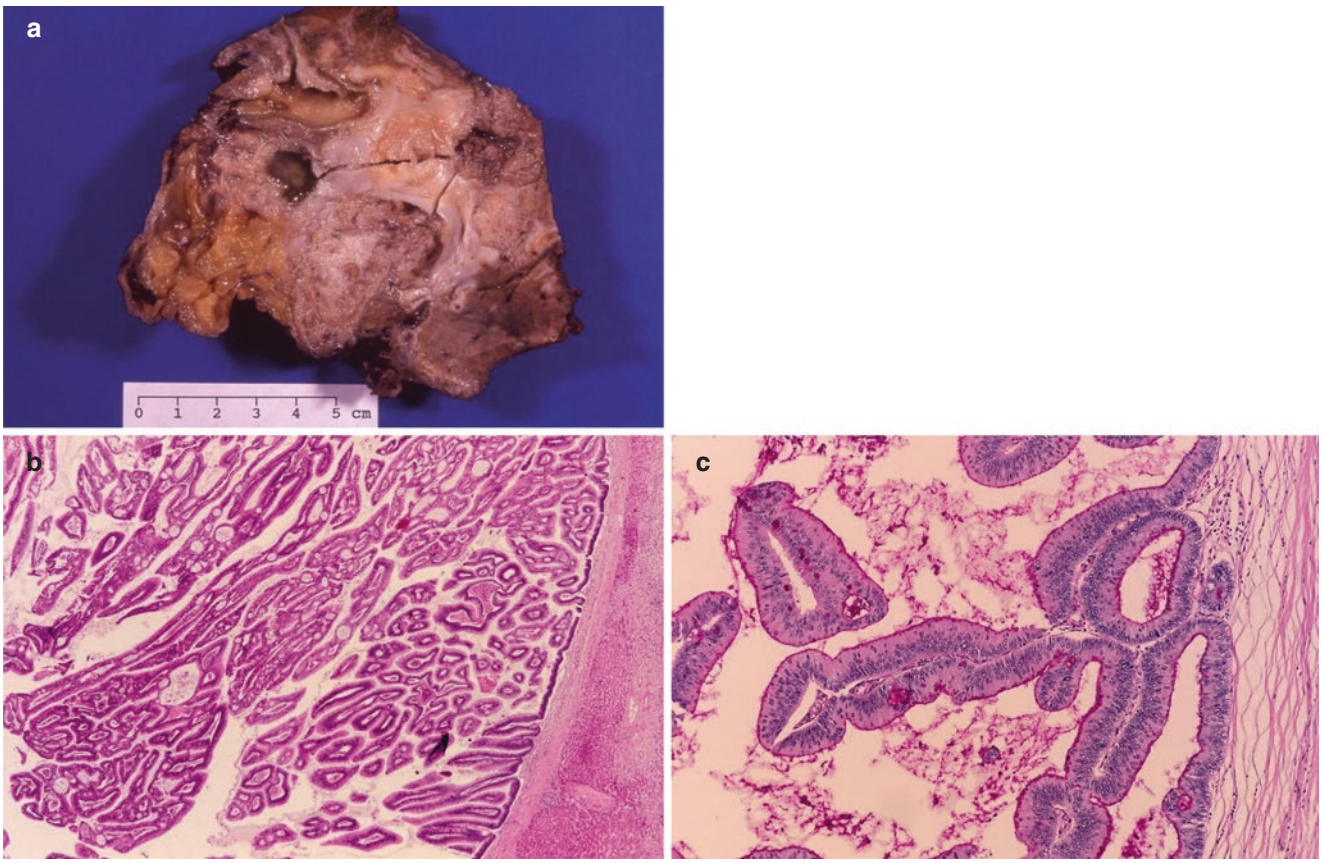


**Fig. 16.15** Intraductal papillary neoplasm (biliary papillomatosis). (**a**) Left hemihepatectomy specimen shows dilated bile ducts filled with papillary tumors. (**b**) Long and branching papillae are lined by columnar cells and supported by delicate fibrovascular stroma. (**c**) The lining epithelium is mucin secreting and dysplastic

**Case 16.8**

A 70-year-old man was found to have liver lesions by US during investigation for epigastric pain. He has undergone biliary surgery 35 years ago. CT revealed markedly dilated intrahepatic bile ducts in atrophic left lobe. After failure of ERCP, left duct PTC was performed and revealed irregular left ducts and a long, irregular, and narrow segment in the proximal part, suggesting a malignant obstruction. FNAC of the left lobe diagnosed biliary papillomatosis, and left hemihepatectomy and right hepaticojejunostomy were performed. The resected specimen revealed papillary tumors filling up the dilated left intrahepatic bile ducts. The ducts contained papillary growth of columnar epithelial cells overlying fibrovascular stalks; the epithelial layer was adenomatous with moderate degree of dysplasia, and apical mucin secretion was present (Fig. 16.15).

## 16.8 Angiomyolipoma and Lipomatous Tumors

A benign mesenchymal tumor, angiomyolipoma (AML) is rare in the liver [41–43]. It contains the same three components as the more commonly encountered renal AML, namely, blood vessels, smooth muscle, and fat. This tumor occurs principally in adults, with a preponderance in females. Only about two-thirds of patients are symptomatic, most commonly with epigastric pain. Rupture with hemoperitoneum rarely occurs in large subcapsular tumors. An association with tuberous sclerosis is recognized in 5–10% of cases; these patients have coexisting renal AML and often have multiple liver tumors. Different ratios of the three components give this tumor its characteristic radiological features.

**Case 16.9**

Routine US in a 67-year-old man showed high-echoic area of 36 mm by 28 mm in S3 (Fig. 16.16). The liver function test was within normal limits, and HBsAg and anti-HCV were negative. Abdominal angiography showed tumor staining in early stage of the arterial phase, and it persisted in late phase (Fig. 16.17). Liver biopsy showed adipose cells admixed with epithelioid and spindle muscle cells and vascular components; fat droplets were also seen in the spindle cells (Fig. 16.18).

An important breakthrough in the understanding of this tumor comes from the documentation of HMB-45 and other melanoma-specific antibodies as reliable markers of AML (Fig. 16.19). Furthermore, recent molecular studies have

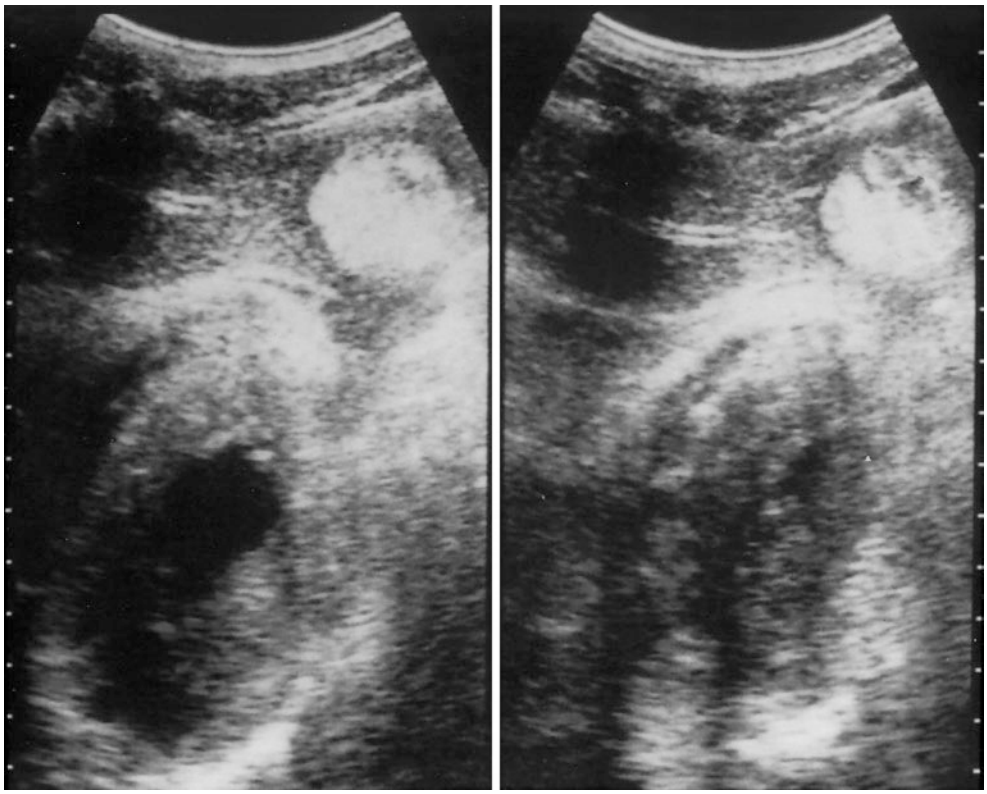

**Fig. 16.16** Angiomyolipoma. US shows high-echoic area mixed with a small, low-echoic area in S3

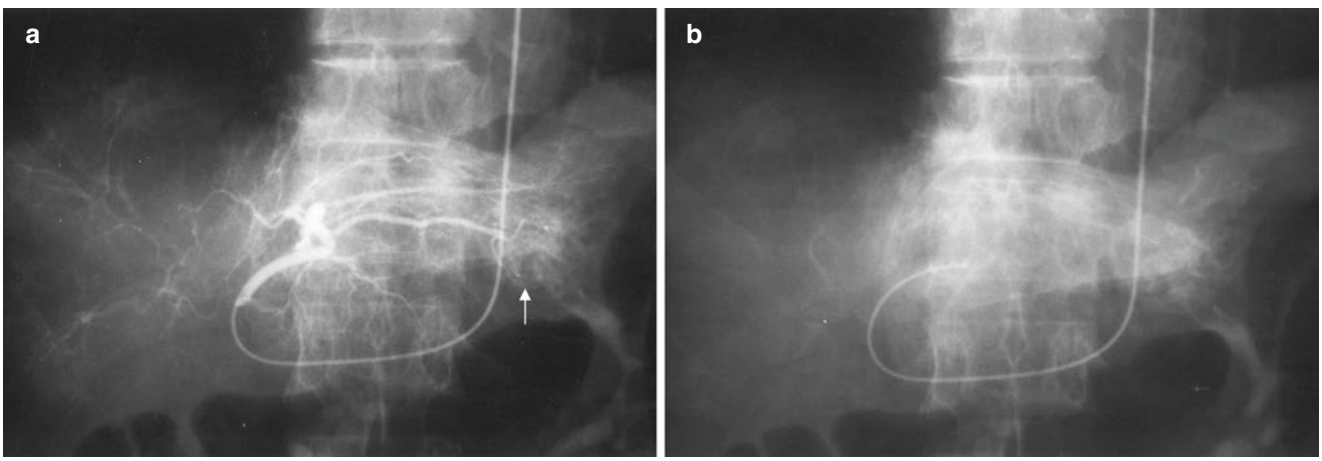


**Fig. 16.17** Angiomyolipoma. (**a**) Angiography shows tumor stain (arrow) in early arterial phase. (**b**) Tumor stain is retained in late stage of arteriography

shown tumor clonality and loss of heterozygosity of tumor suppressor complex genes, indicating a neoplastic process. Once regarded as a hamartomatous lesion, AML is now regarded as a neoplasm belonging to the family of perivascular epithelioid cell tumors (PECOMA) and capable of dual myomatous and lipomatous differentiation and melanogenesis [44]. In most instances, it is a benign tumor, but rare sarcomatous transformation is well documented in renal and liver tumors [45].

AML contains varying proportions of smooth muscle, fat, and blood vessels. Extramedullary hemopoiesis is also frequently present in hepatic tumors, unlike their renal counterpart. According to the line of differentiation and predominance of tissue components, the tumors can be arbitrarily categorized into conventional mixed, lipomatous (>70% fat), myomatous (<10% fat), and angiomatous types [43]. Myomatous AMLs frequently exhibit unusual growth patterns: trabecular, pelioid, and inflammatory (Fig. 16.20).

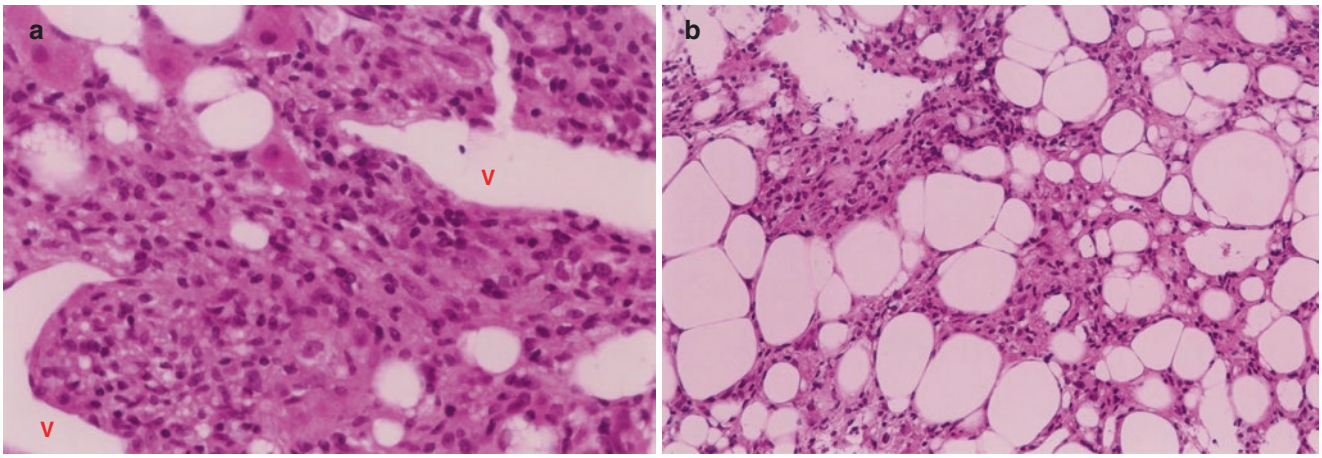


**Fig. 16.18** Angiomyolipoma. (**a**) Adipose cells are admixed with epithelioid muscle cells and vascular components (V). (**b**) Besides adipose cells, fat droplets in spindle-shaped smooth muscle cells are visible

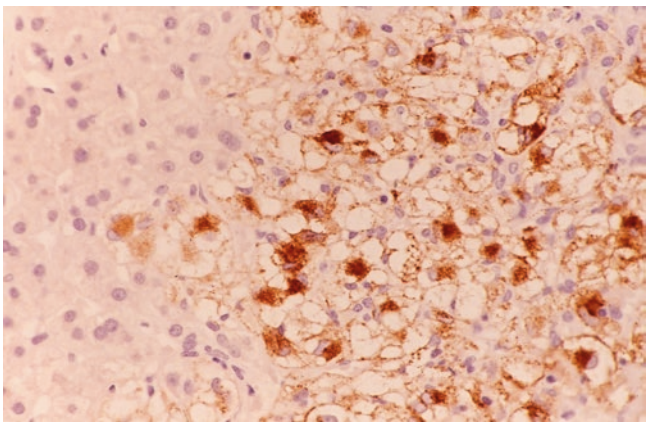

**Fig. 16.19** Angiomyolipoma. Epithelioid cells express intense granular cytoplasmic staining of HMB-45, while hepatocytes are negative

The epithelioid cells may be clear (sugar cell with spiderweb appearance), oncocytic, or pleomorphic. Immunohistochemically, the myoid cells are consistently positive for HMB-45 and other melanogenesis markers; S-100 protein, actin, desmin, and vimentin expression is variable.

Unusual morphologic patterns and cellular features may lead to an erroneous diagnosis, especially of malignancy. Some of the lipomatous tumors reported under the various appellations of lipoma, hibernoma, myelolipoma, and even liposarcoma are all basically AMLs with varying proportions and/or unusual morphology of the different components. Lipomatous AML must be differentiated from focal fatty change, pseudolipoma, true lipoma, and liposarcoma. Myomatous tumors with epithelioid cells are mistaken most frequently for HCC (conventional, clear cell, fibrolamellar types), metastatic renal cell carcinoma, and epithelioid leiomyosarcoma. In AMLs with spindle cells and pleomorphic features, the most common misdiagnosis is some form of sarcoma. The radiological appearance of angiomatous tumors simulates vascular malformation. The diagnosis can be confirmed by a simple panel of immunomarkers, and conservative treatment can be adopted for small tumors after biopsy or FNAC.

## 16.9 Inflammatory Pseudotumor

Inflammatory pseudotumor (IPT) has been described as plasma cell granuloma, pseudolymphoma, fibroxanthoma, and histiocytoma, which reflects the variability of its appearance. Its occurrence in the lung is well known, and IPT is described in almost every other organ and body site. For liver lesions [46–48], there is a 3–1 male preponderance, and most cases occur in children, adolescents, and young adults. However, the age range varies from 10 months to 83 years. Most patients present with recurrent fever, weight loss, and abdominal pain; jaundice develops in a small number of cases. Laboratory investigations reveal neutrophil leukocytosis, a raised erythrocyte sedimentation rate, polyclonal hyperglobulinemia, and, less commonly, anemia, thrombocytopenia, and eosinophilia.

The lesion is solitary in 75% of cases and multiple in remaining cases; in 10% of cases, portal hepatis is involved. The diameter varies from 1 to 25 cm. The cellular composition of IPT varies, perhaps with the age of the lesion. Plump spindle cells with immunohistochemical and ultrastructural findings of myofibroblasts, admixed with polyclonal plasma cells, are consistent features. Lymphocytes, foamy macrophages, neutrophils, and eosinophils are variably present. The stroma is often very vascular and may exhibit a storiform pattern or show sclerosis. Giant-cell granulomas and endophlebitis are rarely observed.

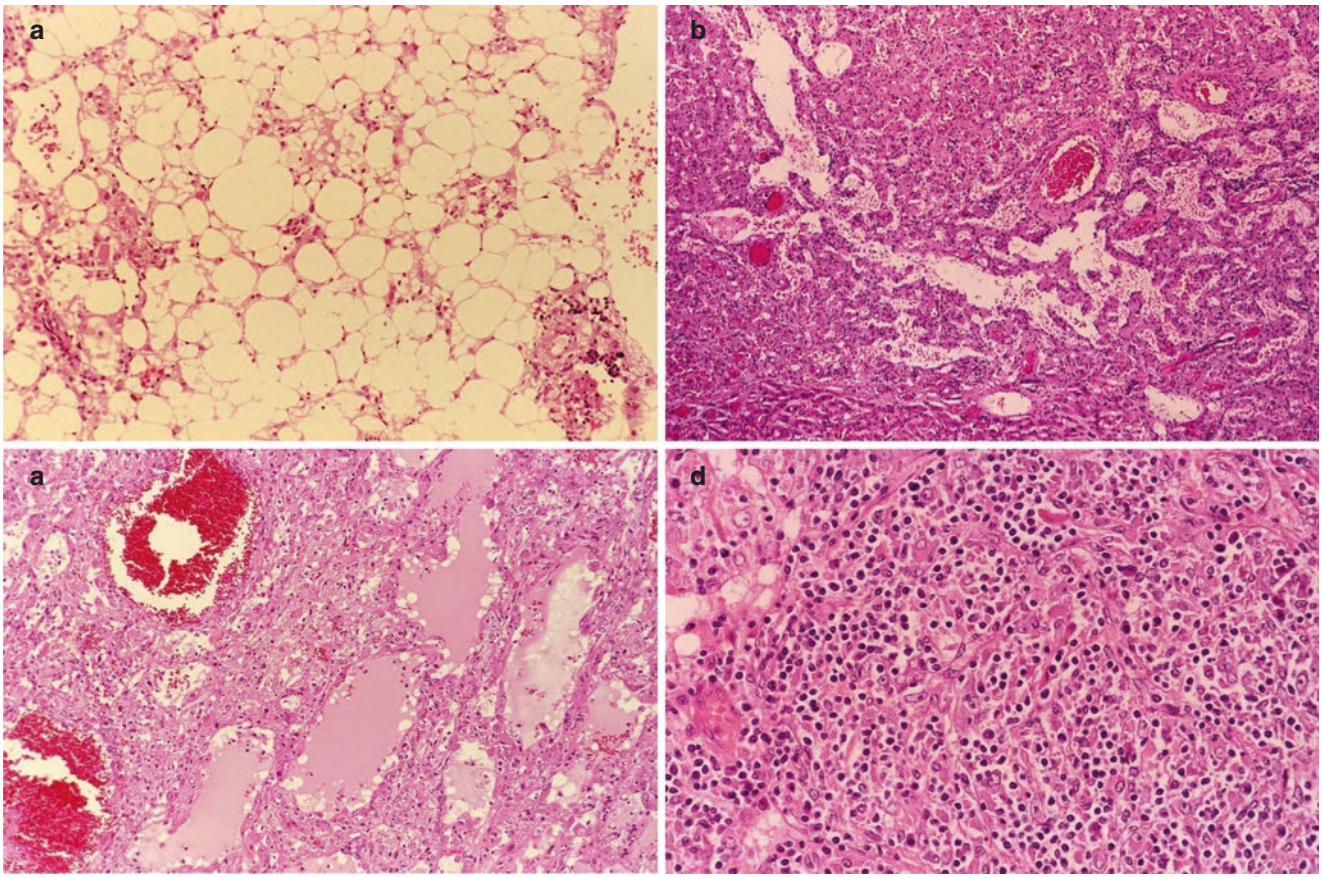


**Fig. 16.20** Angiomyolipoma. (**a**) Lipomatous type AML shows diffuse sheets of adipocytes, with myoid cells webbed between fat cells. (**b**) Pure myomatous AML shows epithelioid cells arranged in trabeculae separated by sinusoids. (**c**) Myomatous AML shows formation of peliotic spaces that are not endothelium-lined. (**d**) AML with an inflammatory pseudotumor-like area, dense lymphoplasmacytic infiltrate, stromal sclerosis, and entrapped short spindle myoid cells

The etiology of IPT is unknown, although the myofibroblastic nature of spindle cells is well established. Very likely, it is a heterogeneous lesion, and various infectious or inflammatory causes have been proposed.

Complete recovery after surgery is the norm, except when major bile ducts are involved, in which case there may be persisting problems with obstructive jaundice, portal hypertension, or malabsorption. Spontaneous resolution, with or without treatment (steroids, antibiotics), is seen in 10% of cases.

### Case 16.10

A 58-year-old man showed low-echoic space-occupying lesions mixed with isoechoic area in S5 (Fig. 16.21). CT with contrast medium showed low-density area; no staining was visible in late phase, and ambiguous low-density area remained (Fig. 16.22). T1-intensified image on MRI showed tumor with low intensity, and T2-intensified image revealed high intensity in tumor (Fig. 16.23). Angiography did not

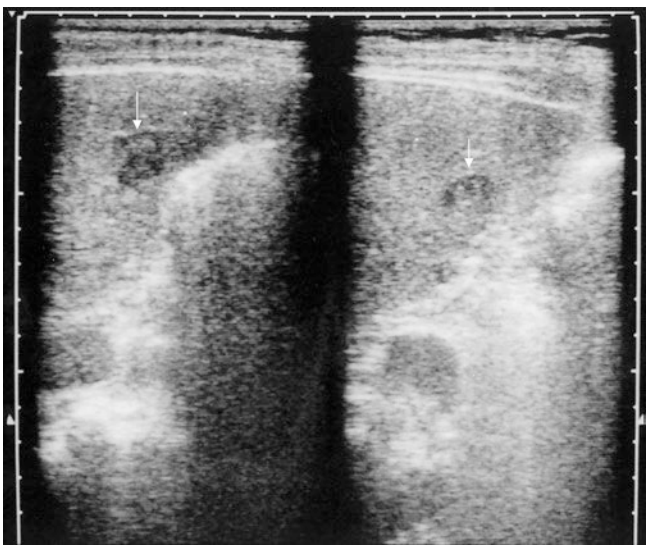

**Fig. 16.21** Inflammatory pseudotumor. US shows low-echoic lesion (arrow) in S5; the edge is sharply defined

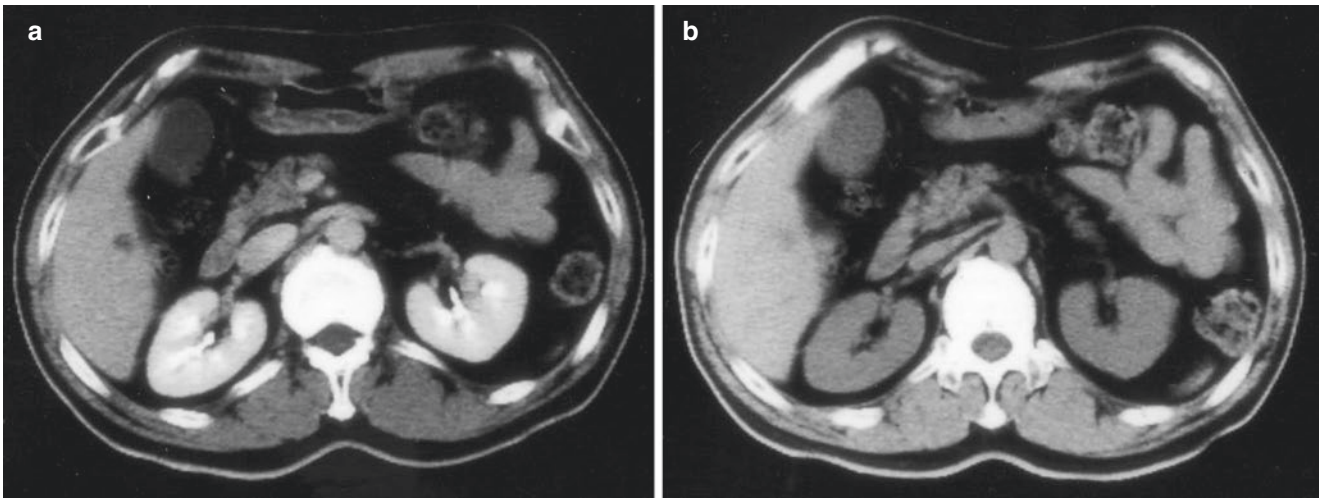


**Fig. 16.22** Inflammatory pseudotumor. (**a**) CT with contrast medium shows sharp, low-density area. (**b**) CT without contrast medium shows ambiguous low-density area

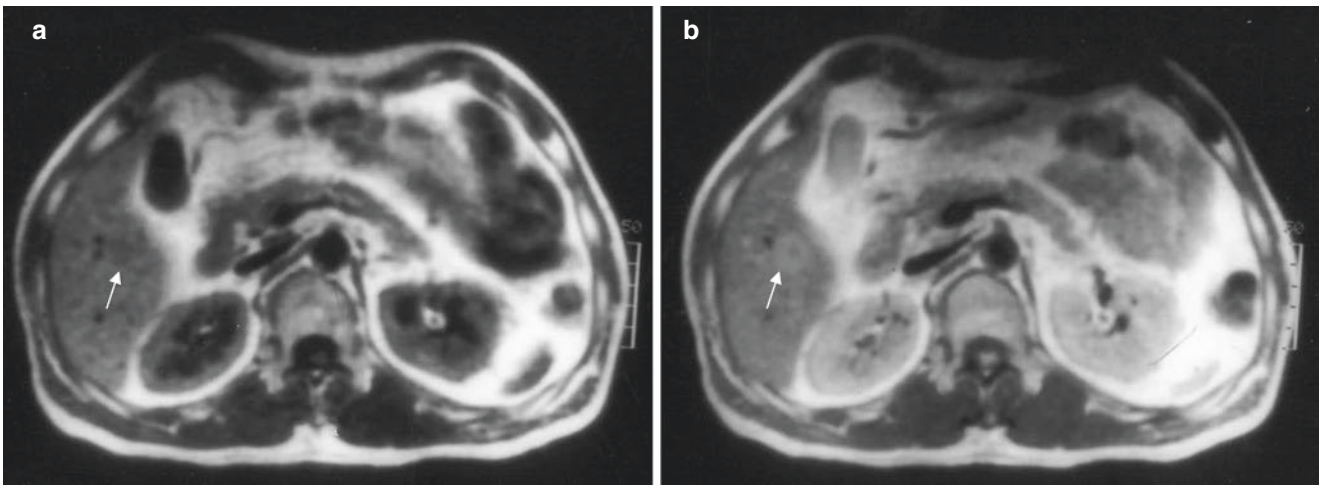


**Fig. 16.23** Inflammatory pseudotumor. (**a**) T1-intensified image on MRI shows low-intensity area (arrow) in S5. (**b**) T2-intensified image on MRI shows high intensity in tumor (arrow)

reveal tumor staining in arterial stage; this was detected in venous phase (Fig. 16.24). Surgical resection of tumor revealed necrotic area surrounded by fibrous bands with a cluster of inflammatory cells; fibrous area showed small vessels, spindle fibroblasts, infiltrating macrophages, lymphocytes, and plasma cells (Fig. 16.25).

Lately, IgG4-related disease is found to form an important cause of IPT and responds to steroid therapy [49]. The lymphoplasmacytic type features perihilar fibroblastic mass with marked lymphoplasmacytic infiltration, prominent eosinophils, numerous IgG4-positive plasma cells, dense fibrosis of hilar and extrahepatic bile ducts (sclerosing cholangitis), and obliterative phlebitis (Fig. 16.26a). Fibrohistiocytic type is characterized by peripheral location, xanthogranulomatous inflammation, neutrophilic infiltration, and obliterated vessels (Fig. 16.26b) [50].

Clinical presentation and gross appearance of hepatic IPT may mimic malignant tumors, and these lesions may be mistaken for sarcoma if attention is not paid to the lack of nuclear atypia exhibited by the spindle cells. More commonly, other neoplasms with an inflammatory cell infiltrate are misdiagnosed as IPT. Examples include follicular dendritic tumor harboring Epstein-Barr virus [51], inflammatory myofibroblastic tumor or low-grade inflammatory fibrosarcoma [52], and inflammatory type of AML [41].

## 16.10 Gauzeoma

A retained foreign body is an uncommon, but not unknown, occurrence after surgical operation. Most patients are symptomatic, and the foreign body is detected by CT and US [53, 54].

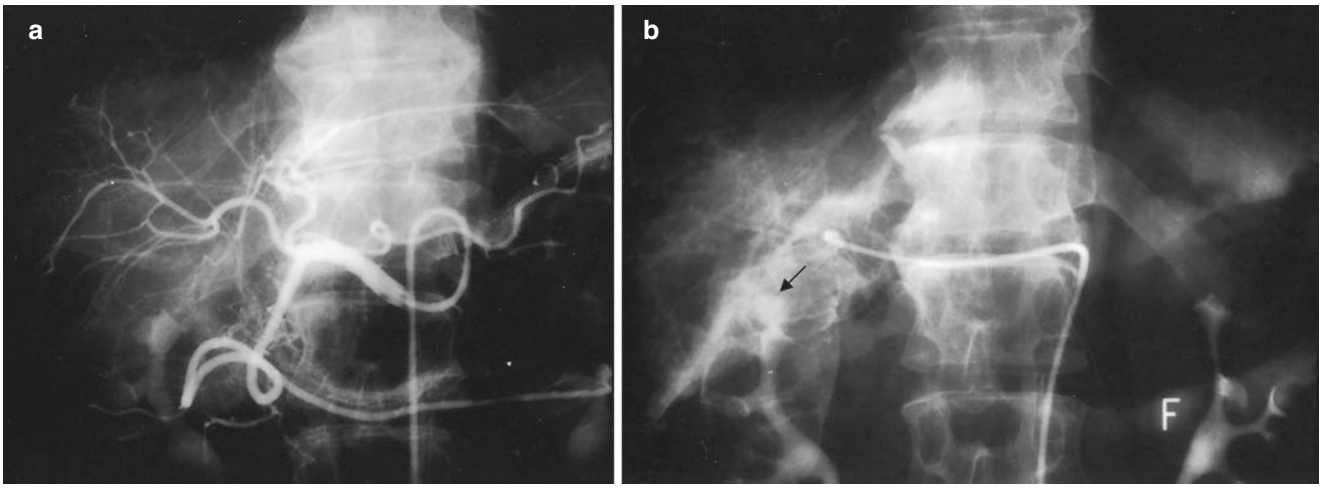


**Fig. 16.24** Inflammatory pseudotumor. (**a**) Tumor cannot be detected in arterial phase of angiography. (**b**) Tumor stain (arrow) is seen in late phase of arteriography

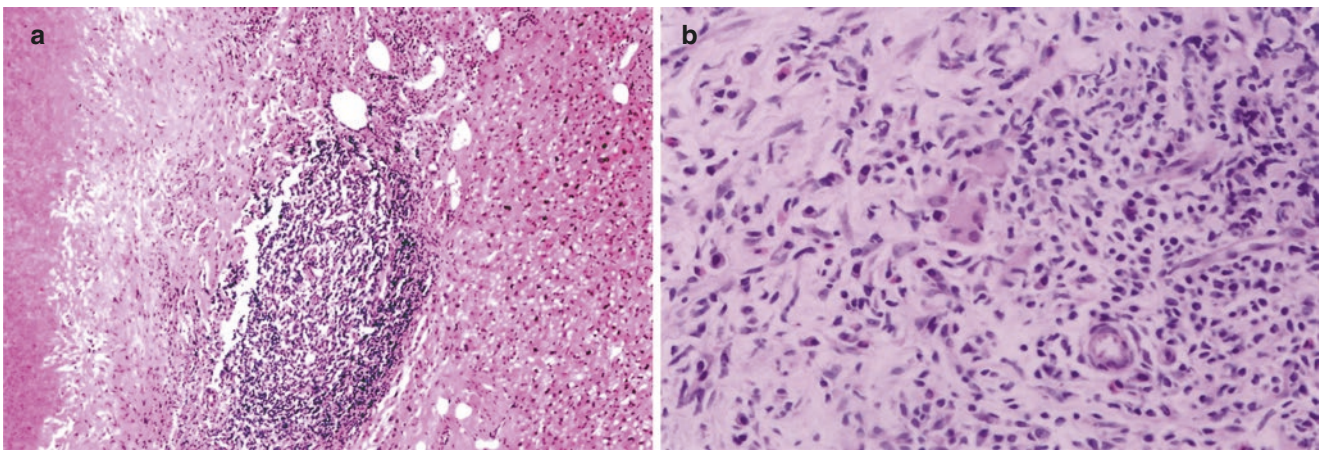


**Fig. 16.25** Inflammatory pseudotumor. (**a**) Necrotic tissue is surrounded by fibrous tissue with clusters of inflammatory cells. Small vessels are seen in the outer fibrotic layer. (**b**) Infiltration of macrophages, lymphocytes, and plasma cells mixed with small vessels are observed in inflammatory area

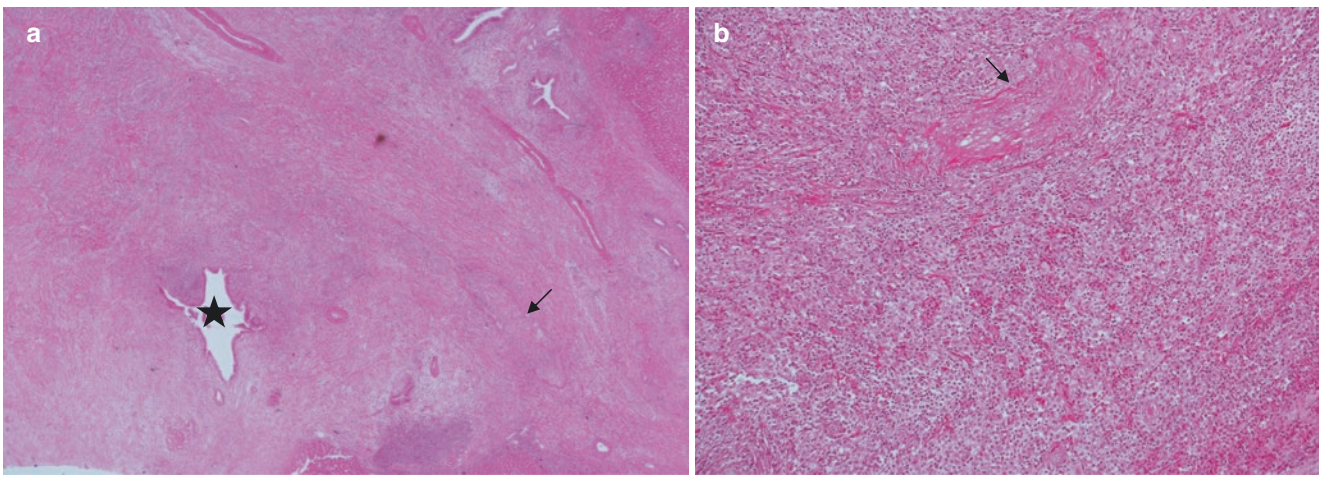


**Fig. 16.26** Inflammatory pseudotumor. (**a**) Lymphoplasmacytic type features perihilar fibroblastic mass with marked lymphoplasmacytic infiltration, dense fibrosis of hilar bile ducts (asterisk), and obliterative phlebitis (arrow). (**b**) Fibrohistiocytic type is characterized by peripheral location, xanthogranulomatous inflammation, neutrophilic infiltration, and obliterated vessels (arrow)

**Case 16.11**

A patient presented with right hypochondralgia 7 years after cholecystectomy. US showed low-echoic lesion with high-echoic rim (Fig. 16.27). CT without contrast medium showed low-density area with high-density rim, and CT with contrast medium revealed high-density area on the rim and low-density area in the center (Fig. 16.28). The cut surface of the tumor revealed sponge-like formation with hemangiomatous structure, purple string-like material, and small vessels surrounded by fibrous bands. The string-like material was found to be a retained gauze (Fig. 16.29).

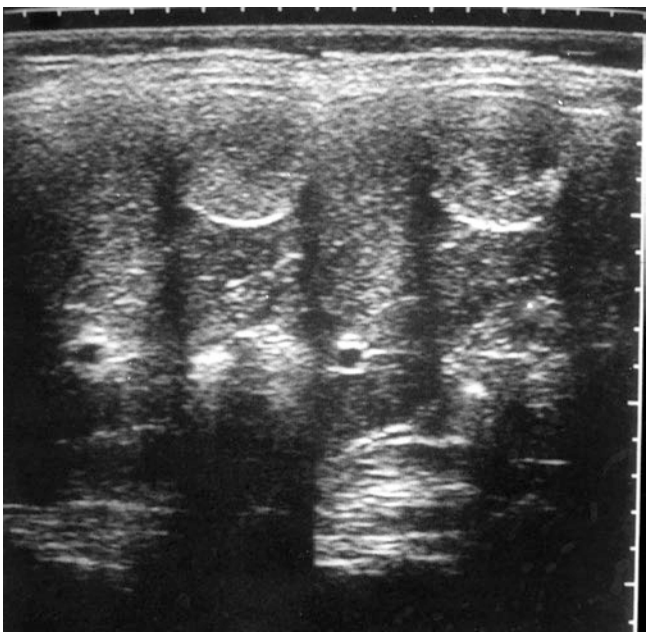

**Fig. 16.27** Gauzeoma. US shows space-occupying lesions with high-echoic rim in S5

## 16.11 Fibrosing Necrotic Nodule

Fibrosing or solitary necrotic nodule of the liver is an uncommon solid lesion. It comprises a central necrotic core enclosed by a hyalinized fibrotic capsule, which contains elastic fibers [55]. These are incidental findings at operation or autopsy.

The lesions are mainly solitary, subcapsular, small, well-demarcated, and round to oval. It has a firm, whitish rim and a core of yellowish white, cheese-like to solid material.

The entity is believed to be a burnt-out phase of a type of benign lesions, and not a lesion having a specific etiology. A small number of cases are claimed to be sclerosed hemangioma [56, 57], but a necrotic center would be unusual. A parasitic origin is documented in those nodules with shadows of degenerated cells, and partially preserved liver reticulin pattern is noted in the necrotic center [58].

**Case 16.12**

A 70-year-old man presented with acute pulmonary edema and a long history of hypertension. Subsequently, he developed left hemiplegia and died. At necropsy, apart from acute myocardial infarction and acute cerebral infarct, a single subcapsular nodule was found on the anterior surface of the left lobe of the liver; the wall of the nodule consisted of dense hyalinized fibrous tissue with elastic fibers and partially obliterated vessels on the outer portion and necrotic material toward the center (Fig. 16.30). There was no granulomatous inflammation or eosinophilic infiltrate.

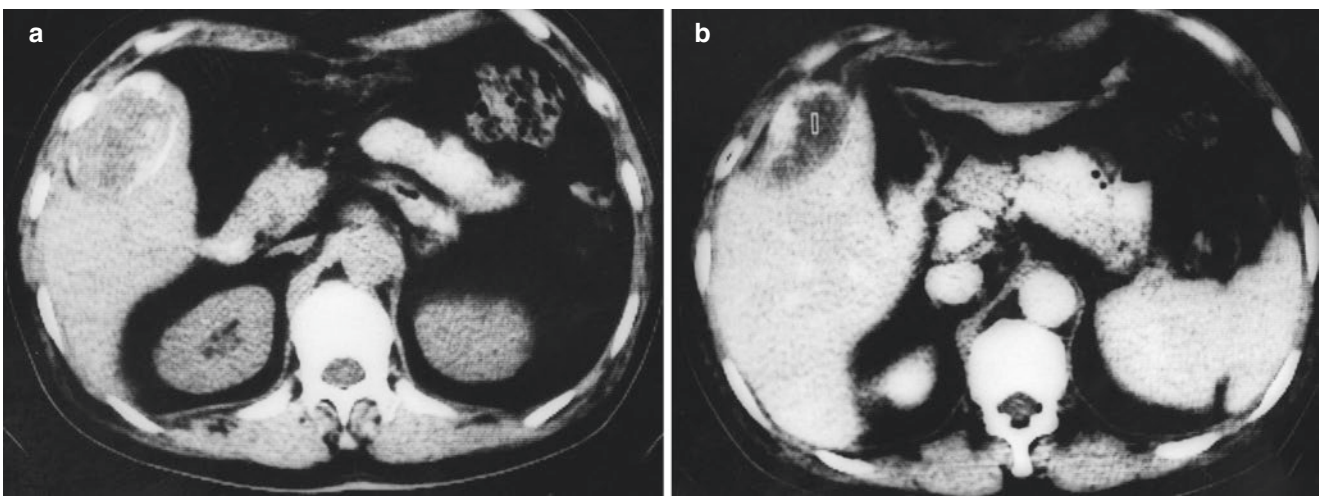


**Fig. 16.28** Gauzeoma. (**a**) CT without contrast medium shows low-density area with high-density rim. (**b**) CT with contrast medium reveals low-density area, and rim is enhanced in scattered fashion

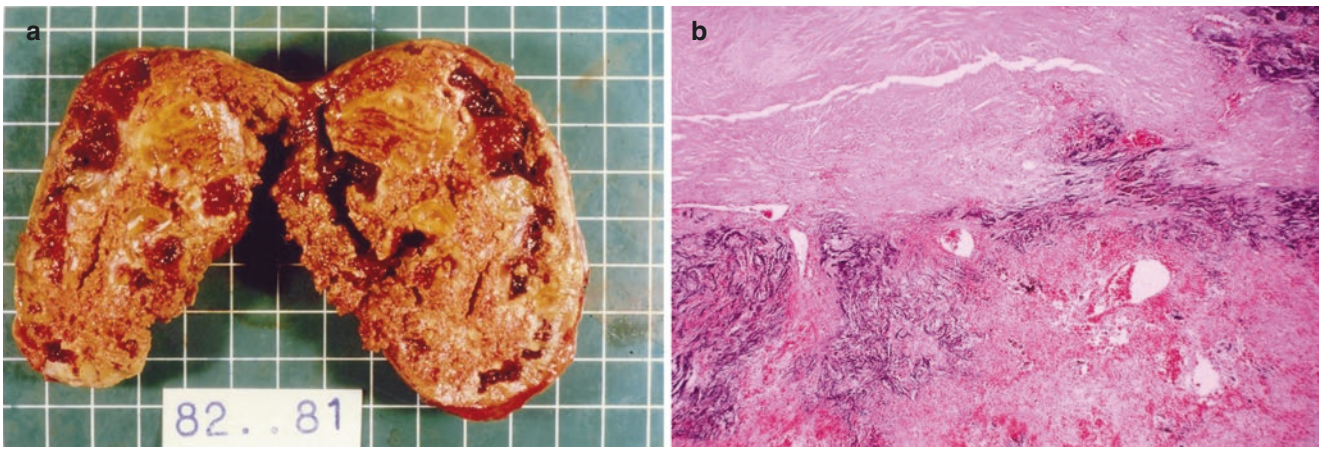


**Fig. 16.29** Gauzeoma. (**a**) Tumor is encapsulated with sponge-like interior. (**b**) Outer surface of tumor comprises fibrous bands mixed with purple strings and small vessels. The inner part is mixed with small vessels, extravasated blood cells, and fibrous strands with purple strings

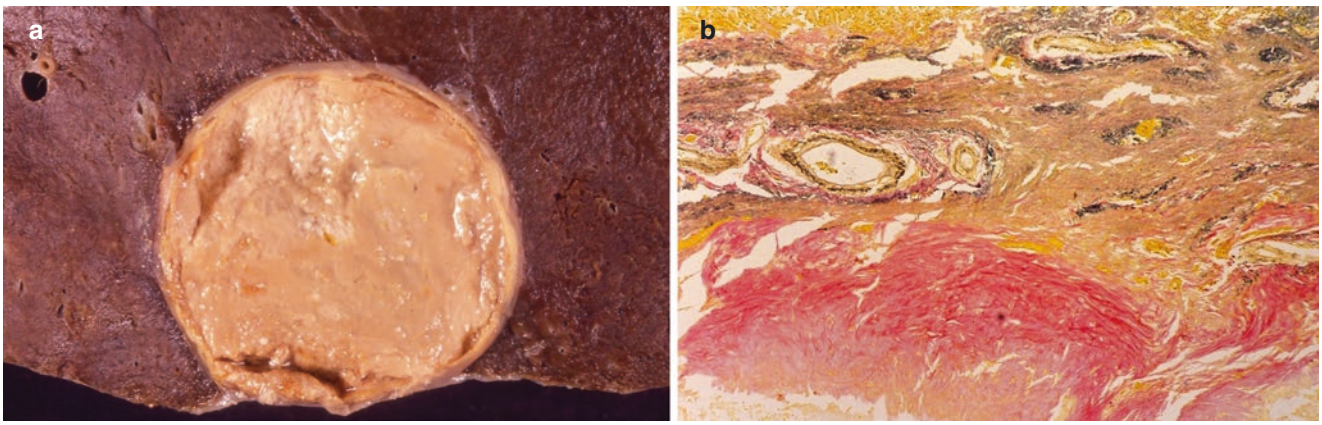


**Fig. 16.30** Fibrosing necrotic nodule. (**a**) Postmortem liver shows well-circumscribed, subcapsular nodule with amorphous, yellowish center. (**b**) Elastic van Gieson stain shows densely fibrotic wall of nodule with elastic fibers, partially obliterated vessels on the outer aspect, and necrotic material toward the center

## 16.12 Parasitic Granuloma

Various kinds of parasites can cause larva migrans syndrome (LMS) [59, 60], and *Toxocara* and *Ascaris* are the most popular culprits [61, 62]. LMS due to *Toxocara canis* or *Toxocara cati* is considered to be common in children of Europe and North America [63] but is reported to be more in number among adults of Japan [62]. After ingesting embryonated egg-contaminated vegetables and eating raw/undercooked paratenic host meat, such as chicken, pig, and beef, humans acquire the infection through intestinal mucosa. Larvae migrate to various tissues and organs through blood or lymph vessels, eliciting immune responses with eosinophilic inflammation. Typical target organs are the liver and lungs, and eyes, brain, and spinal cord may also be affected [63, 64]. Patients with LMS are sometimes asymptomatic or present with fever, abdominal pain, probably due to hepatosplenomegaly, as well as coughing and asthma caused by parasitic pneumonia or bronchitis. Neural or ocular signs are sometimes detected. Hepatic lesions can be detected with various imaging techniques; US shows low echo of space-occupying lesions (about 1 cm in diameter) in the liver [65, 66]; CT reveals low-density area, of which the edge is enhanced by contrast medium; and MRI intensified by T1 presents iso- or low intensity and high intensity by T2. Histopathological examination reveals tumor lesion or granulomas which mainly involve portal tracts. There is a central necrotic area or scar surrounded by eosinophils, lymphocytes, histiocytes, and plasma cells [67, 68]. The most commonly used diagnostic methods are serological techniques such as the enzyme-linked immunosorbent assay (ELISA) or Western blot [69, 70]. Albendazole, mebendazole, or ivermectin is administered

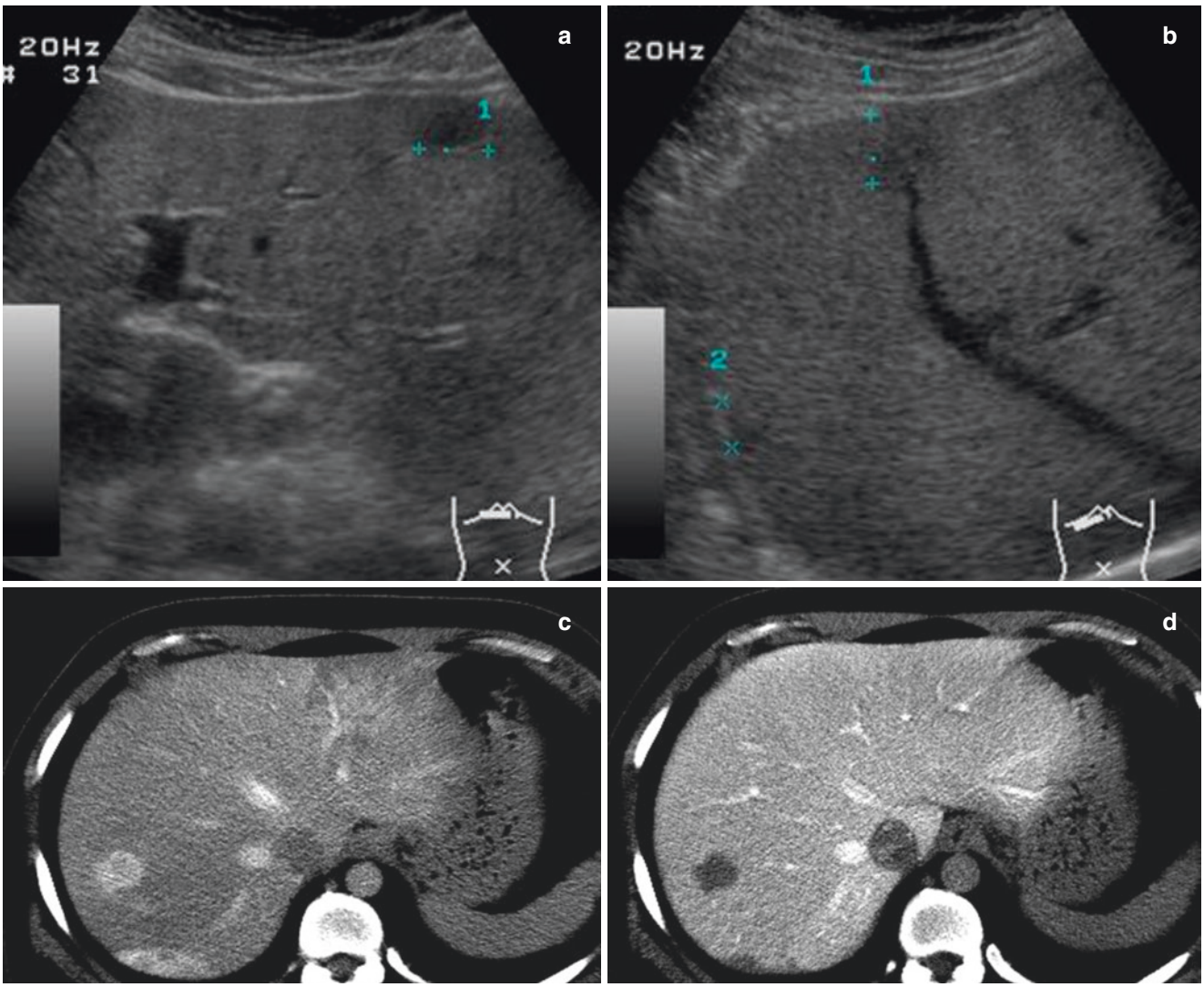


**Fig. 16.31** Parasitic granuloma. (**a** and **b**) Many low-echoic areas (about 1 cm in diameter) are seen near liver surface. (**c**) CTA shows high density area in tumors. (**d**) CTAP shows low-density area in tumors

for treatment of ascariasis and toxocariasis, and piperazine can be used for intestinal obstruction due to their infection [71].

**Case 16.13**

A 34-year-old female was referred for investigation of anti-HCV-positive serum, and her laboratory test showed TBIL 0.4 mg/dL, AST 22 IU/L, ALP 180 IU/L, WBC 11,500/μL, eosinophilic leukocyte 28%, IgE 8200 IU/mL, and CA19-9 44 U/mL. Abdominal US showed multiple low-echoic areas (about 1 cm) near the liver surface (Fig. 16.31). CTA showed high density in tumor-like lesions detected by US, and CTAP showed low-density area. Surgical liver specimen revealed multiple white lesions transparently seen from the surface. Microscopic examination showed nodular formation with central scar surrounded by proliferative bile ducts and infiltration of inflammatory cells and granulomatous formation in portal tracts with many inflammatory cells and proliferative bile ducts (Fig. 16.32). There were infiltration of eosinophilic and neutrophilic leukocytes along with lymphocytes and histiocytes and proliferative bile ducts accompanied by small arterial vessels. ELISA assay confirmed positive reaction for *Ascaris suis*.

**Acknowledgment** Prof. Alex Y. Chang was a coauthor of the first edition of this chapter.

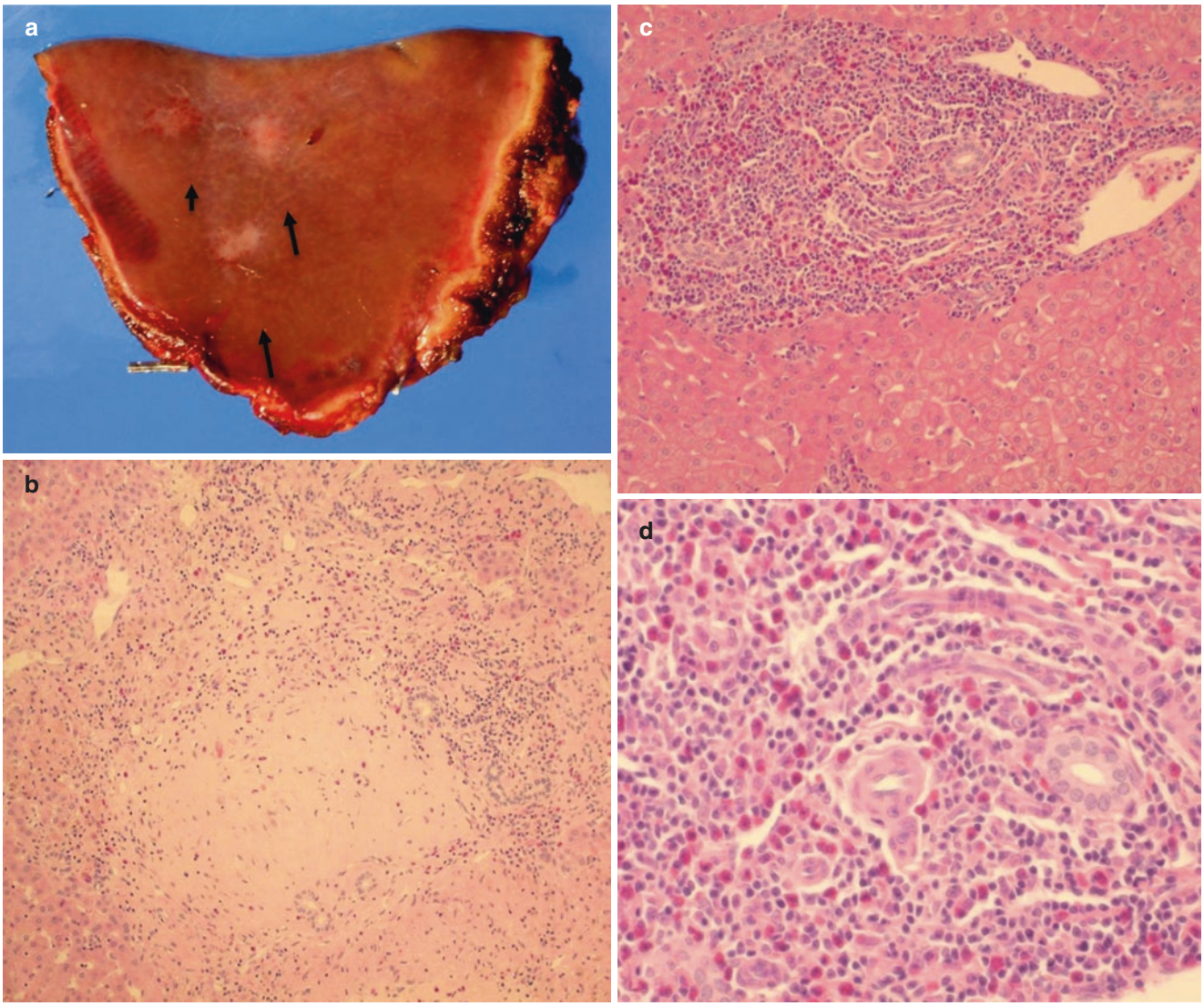


**Fig. 16.32** Parasitic granuloma. (**a**) White-colored nodules are apparent from surface of resected liver. (**b**) Nodular lesion shows central scar surrounded by proliferated bile ductules and inflammatory infiltrate. (**c**) There is granuloma formation in portal tract with dense inflammatory infiltrate. (**d**) Many eosinophils, lymphocytes, and histiocytes are present in the granuloma, admixed with bile ductules and small arterioles

## References

1. Goodman ZD. Benign tumors of the liver. In: Okuda K, Ishak KG, editors. Neoplasms of the liver. Berlin: Springer; 1988. p. 105–25.
2. Bosman FT, Carneiro F, Hruban RH, Theise ND, editors. WHO classification of tumours of the digestive system. 4th ed. Lyon: International Agency for Research on Cancer; 2010.
3. Shimizu M, Miura J, Itoh H, Saitoh Y. Hepatic giant cavernous hemangioma with microangiopathic hemolytic anemia and consumption coagulopathy. Am J Gastroenterol. 1990;85:1411–3.
4. Kim GE, Thung SN, Tsui WM, Ferrell LD. Hepatic cavernous hemangioma: underrecognized associated histologic features. Liver Int. 2006;26:334–8.
5. Lehmann FS, Beglinger C, Schnabel K, Terraciano L. Progressive development of diffuse liver angiomatosis. J Hepatol. 1999; 30:951–4.
6. Ryan RM, Buelow B, Mather C, et al. Hepatic small vessel neoplasm, a rare infiltrative vascular neoplasm of uncertain malignant potential. Hum Pathol. 2016;54:143–51.
7. Song JS, Kim YN, Moon WS. A sclerosing hemangioma of the liver. Clin Mol Hepatol. 2013;19:426–30.
8. Yamashita Y, Shimada M, Taguchi K, Gion T, Hasegawa H, Utsunomiya T, et al. Hepatic sclerosing hemangioma mimicking a metastatic liver tumor: report of a case. Surg Today. 2000;30:849–52.
9. Lee VT, Magnaye M, Tan HW, Thng CH, Ooi LL. Sclerosing haemangioma mimicking hepatocellular carcinoma. Singap Med J. 2005;46:140–3.
10. Makhlouf HR, Ishak KG. Sclerosed hemangioma and sclerosing cavernous hemangioma of the liver: a comparative clinicopathologic and immunohistochemical study with emphasis on the role of mast cells in their histogenesis. Liver. 2002;22: 70–8.

11. Stocker JT, Ishak KG. Focal nodular hyperplasia of the liver: a study of 21 pediatric cases. Cancer. 1981;48:336–45.
12. Paradis V, Laurent A, Flejou JF, Vidaud M, Bedossa P. Evidence for the polyclonal nature of focal nodular hyperplasia of the liver by the study of X chromosome inactivation. Hepatology. 1997;26:891–5.
13. Wanless I, Mawdsley C, Adams R. On the pathogenesis of focal nodular hyperplasia of the liver. Hepatology. 1985;5:1194–200.
14. Nguyen BN, Fléjou JF, Terris B, Belghiti J, Degott C. Focal nodular hyperplasia of the liver: a comprehensive pathologic study of 305 lesions and recognition of new histologic forms. Am J Surg Pathol. 1999;23:1441–54.
15. Paradis V, Benzekri A, Dargère D, Bièche I, Laurendeau I, Vilgrain V, et al. Telangiectatic focal nodular hyperplasia: a variant of hepatocellular adenoma. Gastroenterology. 2004;126:1323–9.
16. Zucman-Rossi J, Jeannot E, Nhieu JT, Scoazec JY, Guettier C, Rebouissou S, et al. Genotype-phenotype correlation in hepatocellular adenoma: new classification and relationship with HCC. Hepatology. 2006;43:515–24.
17. Bioulac-Sage P, Rebouissou S, Thomas C, Blanc JF, Sa Cunha A, Rullier A, et al. Hepatocellular adenoma subtype classification using molecular markers and immunohistochemistry. Hepatology. 2007;46:740–8.
18. Govindarajan S, Peters RL. The bile duct adenoma. A lesion distinct from Meyenburg complex. Arch Pathol Lab Med. 1984;108:922–4.
19. Allaire GS, Rabin L, Ishak KG, Sesterhenn IA. Bile duct adenoma: a study of 152 cases. Am J Surg Pathol. 1988;12:708–15.
20. Bhathal PS, Hughes NR, Goodman ZD. The so-called bile duct adenoma is a peribiliary gland hamartoma. Am J Surg Pathol. 1996;20:858–64.
21. Colombari R, Tsui WM. Biliary tumors of the liver. Semin Liver Dis. 1995;15:402–13.
22. Tsui WM, Loo KT, Chow LT, Tse CC. Biliary adenofibroma. A heretofore unrecognized benign biliary tumor of the liver. Am J Surg Pathol. 1993;17:186–92.
23. Varnholt H, Vauthey JN, Dal Cin P, Marsh Rde W, Bhathal PS, Hughes NR, et al. Biliary adenofibroma: a rare neoplasm of bile duct origin with an indolent behavior. Am J Surg Pathol. 2003;27:693–8.
24. Arnason T, Borger DR, Corless C, Hagen C, Iafrate AJ, Makhlouf H, Misdraji J, Sapp H, Tsui WM, Wanless IR, Zuluaga Toro T, Lauwers GY. Biliary adenofibroma of liver: morphology, tumor genetics, and outcomes in 6 cases. Am J Surg Pathol. 2017;41:499–505.
25. Thai E, Dalla Valle R, Evaristi F, Silini EM. A case of biliary adenofibroma with malignant transformation. Pathol Res Pract. 2016;212:468–70.
26. Thompson SM, Zendejas-Mummert B, Hartgers ML, Venkatesh SK, Smyrk TC, Mahipal A, Smoot RL. Malignant transformation of biliary adenofibroma: a rare biliary cystic tumor. J Gastrointest Oncol. 2016;7:E107–12.
27. Albores-Saavedra J, Hoang MP, Murakata LA, Sinkre P, Yaziji H. Atypical bile duct adenoma, clear cell type: a previously undescribed tumor of the liver. Am J Surg Pathol. 2001;25:956–60.
28. Ishak KG, Willis GW, Cummins SD, Bullock AA. Biliary cystadenoma and cystadenocarcinoma: report of 14 cases and review of the literature. Cancer. 1977;39:322–38.
29. Wheeler DA, Edmondson HA. Cystadenoma with mesenchymal stroma (CMS) in the liver and bile ducts. A clinicopathologic study of 17 cases, 4 with malignant change. Cancer. 1985;56:1434–45.
30. Devaney K, Goodman ZD, Ishak KG. Hepatobiliary cystadenoma and cystadenocarcinoma. A light microscopic and immunohistochemical study of 70 patients. Am J Surg Pathol. 1994;18:1078–91.
31. Subramony C, Herrera GA, Turbat-Herrera EA. Hepatobiliary cystadenoma. A study of five cases with reference to histogenesis. Arch Pathol Lab Med. 1993;117:1036–42.
32. Terada T, Kitamura Y, Ohta T, Nakanuma Y. Endocrine cells in hepatobiliary cystadenomas and cystadenocarcinomas. Virchows Arch. 1997;430:37–40.
33. Kim YI, Kim ST, Lee GK, Choi BI. Papillary cystic tumor of the liver. Cancer. 1990;65:2740–6.
34. Nakanuma Y, Sasaki M, Terada T, Harada K. Intrahepatic peribiliary glands of humans. II. Pathological spectrum. J Gastroenterol Hepatol. 1994;9:80–6.
35. Madden JJ Jr, Smith GW. Multiple biliary papillomatosis. Cancer. 1974;34:1316–20.
36. Chen TC, Nakanuma Y, Zen Y, Chen MF, Jan YY, Yeh TS, et al. Intraductal papillary neoplasia of the liver associated with hepatolithiasis. Hepatology. 2001;34:651–8.
37. Kim YS, Myung SJ, Kim SY, Kim HJ, Kim JS, Park ET, et al. Biliary papillomatosis: clinical, cholangiographic and cholangioscopic findings. Endoscopy. 1998;30:763–7.
38. Tsui WM, Lam PW, Mak CK, Pay KH. Fine-needle aspiration cytologic diagnosis of intrahepatic biliary papillomatosis (intraductal papillary tumor): report of three cases and comparative study with cholangiocarcinoma. Diagn Cytopathol. 2000;22:293–8.
39. Nakanuma Y, Sasaki M, Ishikawa A, Tsui W, Chen TC, Huang SF. Biliary papillary neoplasm of the liver. Histol Histopathol. 2002;17:851–61.
40. Rambaud S, Nores JM, Meeus F, Paolaggi JA. Malignant papillomatosis of the bile ducts: a new indication for liver transplantation? Am J Gastroenterol. 1989;84:448–9.
41. Goodman ZD, Ishak KG. Angiomyolipomas of the liver. Am J Surg Pathol. 1984;8:745–50.
42. Nonomura A, Mizukami Y, Kadoya M, Matsui O, Shimizu K, Izumi R. Angiomyolipoma of the liver: a collective review. J Gastroenterol. 1994;29:95–105.
43. Tsui WM, Colombari R, Portmann BC, Bonetti F, Thung SN, Ferrell LD, et al. Hepatic angiomyolipoma: a clinicopathologic study of 30 cases and delineation of unusual morphologic variants. Am J Surg Pathol. 1999;23:34–48.
44. Bonetti F, Pea M, Martignoni G, Zamboni G. The perivascular epithelioid cell and related lesions. Adv Anat Pathol. 1997;4:343–58.
45. Nguyen TT, Gormann B, Shileds D, Goodman Z. Malignant hepatic angiomyolipoma: report of case and review of literature. Am J Surg Pathol. 2008;32:793–8.
46. Anthony PP, Telesinghe PU. Inflammatory pseudotumour of the liver. J Clin Pathol. 1986;39:761–8.
47. Horiuchi R, Uchida T, Kojima T, Shikata T. Inflammatory pseudotumor of the liver. Clinicopathologic study and review of the literature. Cancer. 1990;65:1583–90.
48. Shek TW, Ng IO, Chan KW. Inflammatory pseudotumor of the liver. Report of four cases and review of the literature. Am J Surg Pathol. 1993;17:231–8.
49. Zen Y, Harada K, Sasaki M, Sato Y, Tsuneyama K, Haratake J, et al. IgG4-related sclerosing cholangitis with and without hepatic inflammatory pseudotumor, and sclerosing pancreatitis-associated sclerosing cholangitis: do they belong to a spectrum of sclerosing pancreatitis? Am J Surg Pathol. 2004;28:1193–203.
50. Zen Y, Fujii T, Sato Y, Masuda S, Nakanuma Y. Pathological classification of hepatic inflammatory pseudotumor, with respect to IgG4-related disease. Mod Pathol. 2007;20:884–94.
51. Selves J, Meggetto F, Brousset P, Voigt JJ, Pradère B, Grasset D, et al. Inflammatory pseudotumor of the liver. Evidence for follicular dendritic reticulum cell proliferation associated with clonal Epstein-Barr virus. Am J Surg Pathol. 1996;20:747–53.
52. Su LD, Atayde-Perez A, Sheldon S, Fletcher JA, Weiss SW. Inflammatory myofibroblastic tumor: cytogenetic evidence supporting clonal origin. Mod Pathol. 1998;11:364–8.

53. Gonzalez-Ojeda A, Rodriguez-Alcantar DA, Arenas-Marquez H, Sanchez Perez-Verdia E, Chavez-Perez R, Alvarez-Quintero R, et al. Retained foreign bodies following intra-abdominal surgery. Hepatogastroenterology. 1999;46:808–12.
54. Kalovidouris A, Kehagias D, Moulopoulos L, Gouliamos A, Pentea S, Vlahos L. Abdominal retained surgical sponges: CT appearance. Eur Radiol. 1999;9:1407–10.
55. Shepherd NA, Lee G. Solitary necrotic nodules of the liver simulating hepatic metastases. J Clin Pathol. 1983;36:1181–3.
56. Berry CL. Solitary "necrotic nodule" of the liver: a probable pathogenesis. J Clin Pathol. 1985;38:1278–80.
57. Sundaresan M, Lyons B, Akosa AB. "Solitary" necrotic nodules of the liver: an aetiology reaffirmed. Gut. 1991;32:1378–80.
58. Tsui WM, Yuen RW, Chow LT, Tse CC. Solitary necrotic nodule of the liver: parasitic origin? J Clin Pathol. 1992;45:975–8.
59. Feldmeier H, Schuster A. Mini review: hookworm-related cutaneous larva migrans. Eur J Clin Microbiol Infect Dis. 2012;31:915–8.
60. Liu Q, Li MW, Wang ZD, Zhao GH, Zhu XQ. Human sparganosis, a neglected food borne zoonosis. Lancet Infect Dis. 2015;15:1226–35.
61. Macpherson CN. The epidemiology and public health importance of toxocariasis: a zoonosis of global importance. Int J Parasitol. 2013;43:999–1008.
62. Maruyama H, Nawa Y, Noda S, Mimori T, Choi WY. An outbreak of visceral larva migrans due to *Ascaris suum* in Kyushu, Japan. Lancet. 1996;347:1766–7.
63. Despommier D. Toxocariasis: clinical aspects, epidemiology, medical ecology, and molecular aspects. Clin Microbiol Rev. 2003;16:265–72.
64. Pinelli E, Herremans T, Harms MG, Hoek D, Kortbeek LM. *Toxocara* and *Ascaris* seropositivity among patients suspected of visceral and ocular larva migrans in the Netherlands: trends from 1998 to 2009. Eur J Clin Microbiol Infect Dis. 2011;30:873–9.
65. Baldisserotto M, Conchin CF, Soares Mda G, Araujo MA, Kramer B. Ultrasound findings in children with toxocariasis: report on 18 cases. Pediatr Radiol. 1999;29:316–9.
66. Ishibashi H, Shimamura R, Hirata Y, Kudo J, Onizuka H. Hepatic granuloma in toxocaral infection: role of ultrasonography in hypereosinophilia. J Clin Ultrasound. 1992;20:204–10.
67. Parsons JC, Bowman DD, Grieve RB. Tissue localization of excretory-secretory antigens of larval Toxocara canis in acute and chronic murine toxocariasis. Am J Trop Med Hyg. 1986;27:492–8.
68. Kaplan KJ, Goodman ZD, Ishak KG. Eosinophilic granuloma of the liver: a characteristic lesion with relationship to visceral larva migrans. Am J Surg Pathol. 2001;25:1316–21.
69. de Savigny DH, Volle A, Woodruff AW. Toxocariasis: serological diagnosis by enzyme immunoassay. J Clin Pathol. 1979;32:284–8.
70. Magnaval JF, Fabre R, Maurieres P, Charlet JP, de Larrard B. Application of the western blotting procedure for the immunodiagnosis of human toxocariasis. Parasitol Res. 1991;77:697–702.
71. Khuroo MS. Ascariasis. Gastroenterol Clin North Am. 1996;25:553–77.